

Ludwig Biermann Award Lecture

The Silent Majority Jets and Radio Cores from Low-Luminosity Black Holes

Heino Falcke

Max-Planck-Institut für Radioastronomie
Auf dem Hügel 69, 53121 Bonn, Germany
hfalcke@mpifr-bonn.mpg.de,
<http://www.mpifr-bonn.mpg.de/staff/hfalcke>

Abstract

They are weak, they are small, and they are often overlooked, but they are numerous and an ubiquitous sign of accreting black holes: compact radio cores and jets in low-power AGN. Here I summarize our work concerning these radio cores and jets in recent years, specifically focusing on the large population of low-luminosity AGN. Special attention is also given to Sgr A, the supermassive black hole candidate at the Galactic Center, whose radio properties are reviewed in more detail. This source exhibits a submm-bump, possibly from an ultra-compact region around the black hole which should allow imaging of the event horizon of the black hole in the not too distant future. A jet model is proposed which explains the basic feature of Sgr A*: its slightly inverted radio spectrum, the submm-bump, the lack of extended emission, and the X-ray emission. This model also works for famous sources like M81*, NGC4258, or GRS1915+105 based on the argument that radio cores are jets whose emission can be scaled with the accretion power over many orders of magnitude. This scaling is corroborated by the detection of many Sgr A*-like radio cores in nearby Low-Luminosity AGN (LLAGN), some of which show jet structures on the VLBI (Very Long Baseline Interferometry) scale. These cores confirm an AGN origin of about half of the known low-luminosity AGN classified as LINERs and dwarf-Seyferts. It is argued that in fact most of the compact radio emission at centimeter waves in LLAGN is produced by a compact radio jet and not an Advection Dominated Accretion Flow (ADAF). In general one can say that compact radio cores are a genuine feature of AGN, allowing one to precisely pinpoint black holes in many galaxies—not only in luminous quasars.*

1 Introduction

1.1 The Vocal Minority

One of the main subjects for radio astronomers has been the study of extragalactic radio jets. When observed at a higher resolution, many of the first radio sources discovered in the early years of radio astronomy later turned out to be powerful, collimated flows of relativistic plasma (called jets) which were ejected from the nucleus of giant elliptical galaxies. These structures can reach sizes of several million light years and hence extend well beyond their host galaxies into the vastness of intergalactic space. This relative isolation is ideal for studying the physics of astrophysical plasma flows in great detail (see e.g., Bridle & Perley 1984; Bridle et al. 1994; Klein et al. 1994; Marti et al. 1997) and allows us to make some estimates of the properties of the IGM (inter-galactic medium, e.g., Subrahmanyam & Saripalli 1993).

An even more important aspect of radio jets, however, is that they are the largest and most visible sign – literally the "smoking gun" – of Active Galactic Nuclei (AGN). The standard model of an AGN consists of a supermassive black hole at the center of a galaxy (Rees 1984) that accretes matter via an accretion disk (von Weizsäcker 1948; Lüst 1952; Shakura & Sunyaev 1973; Lynden-Bell & Pringle 1974). The inflow of matter in the potential well leads to an enormous energy production that is released through infrared (IR), optical, ultra-violet (UV), and X-ray emission. In a fraction of sources one also sees very strong γ -ray and TeV emission. Some of the energy is then funneled into the relativistic radio jet along the rotation axis of the disk. It was, in fact, the strong radio emission from these jets which first led to the discovery of quasars (3C273, Hazard, Mackey, & Shimmins 1963; Schmidt 1963).

Jets have therefore been studied with great interest over many years and in this time a huge zoo of different jet species has emerged, e.g. FR I&II radio galaxies, compact steep spectrum (CSS) and Gigahertz peaked spectrum (GPS) sources, blazars and BL Lacs (e.g., Urry & Padovani 1995). The main reason why all these radio galaxies and radio-loud quasars have been studied in such detail so far is their large radio flux densities of 100 mJy up to several tens of Jy¹, which makes them easily accessible with current technology. On the other hand, it was noted early on that the majority of quasars and AGN in the universe are *not* radio-loud (Strittmatter et al. 1980; Kellermann et al. 1989) and have in fact a rather low radio flux, despite having very similar optical properties compared to radio-loud quasars². Moreover, classical radio galaxies and radio-loud quasars are among the most luminous AGN we know, corresponding to black holes with the largest masses and the largest accretion rates. Hence, when we discuss the properties of relativistic jets in AGN, we

¹1 Jy = 1 Jansky = 1 Watt m⁻² Hz⁻¹

²This does, however, not exclude that radio-quiet quasars have relativistic jets as well (see Miller, Rawlings, & Saunders 1993; Falcke, Sherwood, & Patnaik 1996; Brunthaler et al. 2000).

usually tend to think exclusively about a relatively small but vocal group of sources. Is this the whole universe, or just the tip of the iceberg? Most likely there are many more, weaker black holes and jets in the universe.

1.2 The Silent Majority

The evidence for supermassive black holes in the nuclei of most galaxies has become much stronger recently. Some of the best cases are the Milky Way (Eckart & Genzel 1997), NGC 4258 (Miyoshi et al. 1995), and a number of other nearby galaxies (Faber et al. 1997; Richstone et al. 1998; Magorrian et al. 1998) where convincing dynamical evidence for black holes exists. Hence, the basic powerhouse for an AGN – the black hole – is built into almost every galaxy, but compared to quasars and radio galaxies there is a huge range in power output between the most luminous quasars and barely active galaxies like the Milky Way.

For example in a spectroscopic survey of 486 nearby bright galaxies, Ho, Filippenko, & Sargent (1997) found that a large fraction of these galaxies have optical emission-line spectra. Roughly one third of the galaxies surveyed showed spectra usually attributed to active galactic nuclei. The energy output of these systems, is $10^{-6} - 10^{-3}$ times lower than in typical quasars (Ho 1999). Consequently, these galaxies are called low-luminosity AGN (LLAGN). The large fraction of LLAGN already indicates that the number of AGN increases with decreasing luminosity. This is just the continuation of a trend that has been found already in studies of the luminosity function of quasars and Seyfert galaxies, namely a power-law distribution of AGN as a function of luminosity with an index $\alpha \simeq -2.2$ (e.g., Köhler et al. 1997, see Fig. 1). As in real life, the majority of the entire population is rather quiet. To get a complete view of the astrophysics of AGN and black holes one therefore needs to look at this silent majority as well.

The question of how the central engines in quasars and low-luminosity AGN are related to each other and why they appear so different despite being powered by the same type of object is therefore of major interest. For many nearby galaxies with low luminosity nuclear emission-lines, it is not even clear whether they are powered by an AGN or by star formation. This is especially true for Low Ionization Nuclear Emission Region (LINER) galaxies (Heckman 1980; Heckman et al. 1983), some of which can be explained in terms of aging starbursts (e.g., Filippenko & Terlevich 1992; Alonso-Herrero et al. 2000).

One of the best ways to probe the very inner parts of these engines is to study the compact radio sources found in many AGN. Indeed, despite their low optical luminosity, quite a few nearby galaxies have such radio sources in their nuclei, prominent cases being the Milky Way (Sgr A*), and the galaxies M 104 and M 81 (Bietenholz et al. 1996). These radio sources resemble the cores of radio-loud quasars, showing a very high brightness temperature and a flat to inverted radio spectrum that extends up to sub-millimeter (submm) wavelengths.

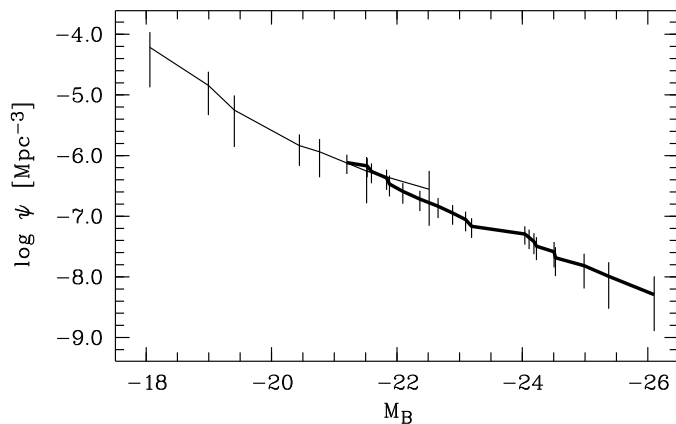


Figure 1: Local luminosity function (number density as a function of absolute magnitude) of $z < 0.3$ quasars and Seyferts. The number of AGN decreases with a power-law index of $\alpha \simeq -2.2$ as the luminosity increases (from Köhler et al. 1997).

1.3 Radio Cores, Jets, and Accretion

What are these compact radio cores and how are they related to the AGN? Early on in the discussion about the existence of black holes, Lynden-Bell & Rees (1971) suggested that they would be accompanied by compact radio nuclei, detectable by Very Long Baseline Interferometry (VLBI), and predicted such a source for the Galactic Center. Indeed, this source (Sgr A*) was then discovered by Balick & Brown (1974) and it became clear in later years that compact radio cores are indeed good evidence for the existence of an AGN or a black hole in a galaxy. For luminous radio galaxies and radio-loud quasars the basic nature of these compact radio nuclei has been clarified in the meantime through extensive and detailed VLBI observations (see Zensus 1997 for a review) as being the inner regions of relativistic jets emanating from the nucleus.

Despite this progress, a number of important questions remain when looking back at the initial discussion. First of all, it is unclear whether there indeed is a direct link between compact radio cores and AGN, i.e. whether compact radio cores and jets are just an accidental by-product of black hole activity or a necessary consequence. Secondly, for the lesser studied, low-luminosity AGN the jet nature of compact radio nuclei has not yet been established beyond any doubt, leaving the question open whether in fact a compact radio core in a low-luminosity AGN is the same as in a high-luminosity AGN, i.e. a quasar.

Such a similarity was exactly the claim made by Falcke & Biermann (1995), stimulated by the seminal paper by Rawlings & Saunders (1991), where it was proposed that accretion disks and jets form symbiotic systems. A scaling law was proposed which connects high-power and lower-power accretion disks and their associated radio jets (cores). Alternatively it was argued that radio cores

in LLAGN could be due to the accretion flow itself if it becomes advection dominated (Narayan & Yi 1994; Narayan & Yi 1995a; Narayan & Yi 1995b). This idea was applied to a range of objects including the Galactic Center (Narayan, Yi, & Mahadevan 1996; see also Rees 1982 and Melia 1994).

The purpose of this work is therefore to describe a comprehensive study of the radio emission from AGN operating at powers less than those of typical quasars and to clarify their nature. By going to lower powers we want to understand how universal the central engine really is. Are radio cores in LLAGN different from those in quasars? How important is the formation of jets at lower power? Are there classes of sources where no jet is found? What happens with the jets in quasars if the power of the engine becomes less and less: Will the jets die completely, implying that accretion near the Eddington limit is required for the jet formation, or will the jet just become proportionally weaker, implying that jet formation is an integral part of accretion physics and independent of the exact nature of the accretion disk itself?

2 The Jet-Disk Symbiosis Model

2.1 Jet-Disk Coupling

In order to quantify the radio emission we expect from a radio jet close to the nucleus we will make a few simple assumptions and resort to the simple Ansatz that every jet is coupled to an accretion disk. A coupled jet-disk system has to obey the same conservation laws as all other physical systems, i.e. at least energy and mass conservation. We can express those constraints by specifying that the total jet power Q_{jet} of the two oppositely directed beams is a fraction $2q_j < 1$ of the accretion power $Q_{\text{disk}} = \dot{M}_{\text{disk}}c^2$, the jet mass loss is a fraction $2q_m < 1$ of the disk accretion rate \dot{M}_{disk} , and the disk luminosity is a fraction $q_l < 1$ of Q_{disk} for a standard optically thick disk ($q_l = 0.05 - 0.3$ depending on the spin of the black hole). The dimensionless jet power q_j and mass loss rate q_m are coupled by the relativistic Bernoulli equation (Falcke & Biermann 1995) for a jet/disk-system. For a large range in parameter space the total jet energy is dominated by the kinetic energy such that one has $\gamma_j q_m \simeq q_j$, in case the jet reaches its maximum sound speed, $c/\sqrt{3}$, the internal energy becomes of equal importance and one has $2\gamma_j q_m \simeq q_j$ ('maximal jet'). The internal energy is assumed to be dominated by the magnetic field, turbulence, and relativistic particles. We will constrain the discussion here to the most efficient type of jet where we have equipartition between the relativistic particles and the magnetic field and also have equipartition between the internal and kinetic energy (i.e. bulk motion) – one can show (see Falcke & Biermann 1995) that other, less efficient models would fail to explain the highly efficient radio-loud quasars.

Knowing the jet energetics, we can describe the longitudinal structure of the jet at first by assuming a constant jet velocity (beyond a certain point) and free expansion according to the maximal sound speed ($c_s \lesssim c/\sqrt{3}$). For

such a jet, the equations become very simple. The magnetic field is given by

$$B_j = 0.3 G Z_{\text{pc}}^{-1} \sqrt{q_{j/1} L_{46}} \quad (1)$$

and the particle number density is

$$n = 11 \text{ cm}^{-3} L_{46} q_{j/1} Z_{\text{pc}}^{-2} \quad (2)$$

(in the jet rest frame). Here Z_{pc} is the distance from the origin in parsec (pc), L_{46} is the disk luminosity in 10^{46} erg/sec, $2q_{j/1} = 2q_j/q_1 = Q_{\text{jet}}/L_{\text{disk}}$ is the ratio between jet power (two cones) and disk luminosity which is of the order 0.1–1 (Falcke, Malkan, & Biermann 1995) and $\gamma_{j,5} = \gamma_j/5$ ($\beta_j \simeq 1$). If one calculates the synchrotron spectrum of such a jet, one obtains locally a self-absorbed spectrum that peaks at

$$\nu_{\text{ssa}} = 20 \text{ GHz } \mathcal{D} \frac{(q_{j/1} L_{46})^{2/3}}{Z_{\text{pc}}} \left(\frac{\gamma_{e,100}}{\gamma_{j,5} \sin i} \right)^{1/3}. \quad (3)$$

Integration over the whole jet yields a flat spectrum with a monochromatic luminosity of

$$L_\nu = 1.3 \cdot 10^{33} \frac{\text{erg}}{\text{s Hz}} (q_{j/1} L_{46})^{17/12} \mathcal{D}^{13/6} \sin i^{1/6} \gamma_{e,100}^{5/6} \gamma_{j,5}^{11/6}, \quad (4)$$

where $\gamma_{e,100}$ is the minimum *electron* Lorentz factor divided by 100, and \mathcal{D} is the *bulk* jet Doppler factor. At a redshift of 0.5 this luminosity corresponds to an un-boosted flux of ~ 100 mJy. The brightness temperature of the jet is

$$T_b = 1.2 \cdot 10^{11} \text{ K } \mathcal{D}^{4/5} \left(\frac{\gamma_{e,100}^2 q_{j/1} L_{46}}{\gamma_{j,5}^2 \beta_j} \right)^{1/12} \sin i^{5/6} \quad (5)$$

which is almost independent of all parameters except the Doppler factor. An important factor that governs the synchrotron emissivity is, of course, the relativistic electron distribution, for which we have assumed a power-law distribution with index $p = 2$ and a ratio 100 between maximum and minimum electron Lorentz factor. As we are discussing here the most efficient jet model we also assume that all electrons are accelerated (i.e. $x_e = 1$ in Falcke & Biermann 1995), hence the only remaining parameter is the minimum Lorentz factor of the electron distribution $\gamma_{e,100}$ determining the total electron energy content. In order to reach the magnetic field equipartition value, which is close to the kinetic jet power governed by the protons, we have to require $\gamma_{e,100} \sim 1$.

Thus, using $L_{\text{disk}} \sim 10^{46}$ erg/sec (typical optical/UV-luminosity) and $\gamma_j \sim 5$ (a few times the escape speed from a black hole), we can easily explain pc-scale radio cores at cm-wavelengths, with brightness temperatures of 10^{11} K and fluxes of 100 mJy and more without any need for a ‘cosmic conspiracy’ (e.g., Cotton et al. 1980).

2.2 UV/Radio Correlation

Now, we will have to validate some of our assumptions and test the jet-disk coupling derived above. To stay on safe grounds we will in this section concentrate on the well-studied quasars. For these sources we have to estimate the disk luminosity as precisely as possible and compare it to their radio cores. The best studied quasar sample so far is the PG quasar sample (Schmidt & Green 1983). For most sources in this sample Sun & Malkan (1989), using optical and IUE data, fitted the UV bump with accretion-disk models and a few more were available in the archive (Falcke, Malkan, & Biermann 1995). There are also excellent photometric (Neugebauer et al. 1987) and spectroscopic data (Boroson & Green 1992) available. Unlike the broadband UV-bump fits, which give L_{disk} directly, emission-lines and continuum colors do not give a direct estimate for the bolometric UV luminosity and L_{disk} . We will need to calibrate those values to obtain an equivalent UV bump luminosity using the sources which have a complete set of data available. This yields

$$\lg(L_{\text{disk}}/\text{erg s}^{-1}) = 2.85 + \lg(L_{[\text{OIII}]}/\text{erg s}^{-1}), \quad (6)$$

$$\lg(L_{\text{disk}}/\text{erg s}^{-1}) = 2.1 + \lg(L_{\text{H}\beta}/\text{erg s}^{-1}), \quad (7)$$

$$\lg(L_{\text{disk}}/\text{erg s}^{-1}) = -0.4M_{\text{b}} + 35.90. \quad (8)$$

Here $L_{[\text{OIII}]}$ and $L_{\text{H}\beta}$ are the luminosities in the $[\text{OIII}]\lambda 5007$ and $\text{H}\beta$ (broad) emission-lines, M_{b} is the absolute blue continuum magnitude as used by Boroson & Green (1992). The scatter in this relation, ~ 0.5 in the log, is shown in Falcke, Malkan, & Biermann (1995).

In Figure 2 we plot the radio core luminosity against the accretion disk luminosity derived from the above relations for a quasar sample. This demonstrates that the *cores* of these quasars show the distribution expected within the jet-disk model, assuming one has relativistic jets in radio-loud *and* radio-quiet quasars operating at two basic levels of efficiency (see Falcke & Biermann 1995 for a discussion of what these basic levels could be). The spread in the radio luminosity distribution is dominated by relativistic boosting and random inclination angles. As expected, flat spectrum radio-loud quasars, with the exception of a few radio-intermediate quasars (possibly boosted radio-quiet quasars, Miller, Rawlings, & Saunders 1993; Falcke, Sherwood, & Patnaik 1996), are found at the highest radio luminosities expected for jets with small inclination angles. This spread can be translated into characteristic bulk Lorentz factors for the jets, yielding a range between $\gamma_{\text{j}} = 3 - 10$.

2.3 Radio Cores in LLAGN: Free Jet with Pressure Gradient

Radio cores in quasars are quite well-studied and therefore one can tolerate a number of free parameters in the jet model which are constrained by additional observations. One of these parameters is the jet speed which is

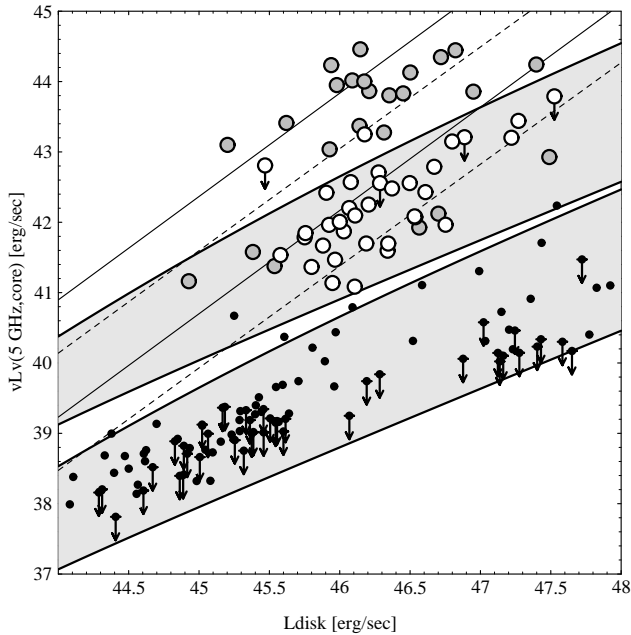


Figure 2: Radio *core* luminosity vs. disk (UV-bump) luminosity for quasars (including a complete optical and a radio-selected sample). The shaded circles are core-dominated, flat-spectrum sources, open circles are steep-spectrum (FR II type) sources, and filled points are radio-quiet sources. The shaded bands represent the radio-loud and radio-quiet jet models where the width is determined by relativistic boosting. The jet velocity evolves with luminosity as $\gamma_j \beta_j \propto L^{0.1}$, as discussed in Falcke, Malkan, Biermann (1995). The dashed lines represent the expected level of emission for sources just within the boosting cone (i.e. inclination $i = 1/\gamma$) and the isolated solid lines represent emission for $i = 0^\circ$ inclination – corresponding to the maximally boosted flux. The position of flat-spectrum and steep-spectrum sources and the radio-loud/radio-quiet separation can be naturally accounted for with the coupled jet-disk model.

generally believed to be in the range $\gamma_{\text{jet}} \sim 5 - 10$ based on the observation of superluminal motion. In LLAGN the situation is different and we have no direct evidence whether they are highly-, moderately-, or sub-relativistic. It is therefore useful to find a self-consistent description of the velocity field in these radio cores mainly based on first principles. One possibly important inconsistency of the basic jet model outlined above, which is based on Blandford & Königl (1979), is that it ignores the effects of any pressure gradients: one can show that a self-consistent treatment implies a weak acceleration of the bulk jet flow due to its longitudinal pressure gradient. This cannot only naturally explain why the radio spectra of some LLAGN radio cores are slightly inverted (e.g., Sgr A* & M81*; see Duschl & Lesch 1994; Reuter & Lesch 1996; Falcke et al. 1998) rather than just flat, it also provides one with a natural velocity field for the jet, taking away γ_{jet} as a free parameter.

All these simplifications lead to the following expressions for the observed flux density and angular size of a radio core observed at a frequency ν as a function of jet power. For a source at a distance D , with black hole mass M_\bullet , size of nozzle region Z_{nozz} (in $R_g = GM_\bullet/c^2$), jet power Q_{jet} , inclination angle i , and characteristic electron Lorentz factor γ_e ³ the observed flux density spectrum is given as (Falcke & Biermann 1999)

$$\begin{aligned}
 S_\nu &= 10^{2.06 \cdot \xi_0} \text{ mJy} \left(\frac{Q_{\text{jet}}}{10^{39} \text{ erg/sec}} \right)^{1.27 \cdot \xi_1} \\
 &\cdot \left(\frac{D}{10 \text{ kpc}} \right)^{-2} \left(\frac{\nu}{8.5 \text{ GHz}} \right)^{0.20 \cdot \xi_2} \left(\frac{M_\bullet}{33 M_\odot} \frac{Z_{\text{nozz}}}{10 R_g} \right)^{0.20 \cdot \xi_2} \\
 &\cdot \left(3.9 \cdot \xi_3 \left(\frac{\gamma_{e,0}}{200} \right)^{-1.4 \cdot \xi_4} - 2.9 \cdot \xi_5 \left(\frac{\gamma_{e,0}}{200} \right)^{-1.89 \cdot \xi_6} \right), \quad (9)
 \end{aligned}$$

with the correction factors ξ_{0-6} depending on the inclination angle i (in radians):

$$\xi_0 = 2.38 - 1.90 i + 0.520 i^2 \quad (10)$$

$$\xi_1 = 1.12 - 0.19 i + 0.067 i^2 \quad (11)$$

$$\xi_2 = -0.155 + 1.79 i - 0.634 i^2 \quad (12)$$

$$\xi_3 = 0.33 + 0.60 i + 0.045 i^2 \quad (13)$$

$$\xi_4 = 0.68 + 0.50 i - 0.177 i^2 \quad (14)$$

$$\xi_5 = 0.09 + 0.80 i + 0.103 i^2 \quad (15)$$

$$\xi_6 = 1.19 - 0.29 i + 0.101 i^2. \quad (16)$$

Likewise, the characteristic angular size scale of the emission region is given by

$$\begin{aligned}
 \Phi_{\text{jet}} &= 1.36 \cdot \chi_0 \text{ mas} \sin i \\
 &\cdot \left(\frac{\gamma_{e,0}}{200} \right)^{1.77 \cdot \chi_1} \left(\frac{D}{10 \text{ kpc}} \right)^{-1} \left(\frac{\nu}{8.5 \text{ GHz}} \right)^{-0.89 \cdot \chi_1} \\
 &\cdot \left(\frac{Q_{\text{jet}}}{10^{39} \text{ erg/sec}} \right)^{0.60 \cdot \chi_1} \left(\frac{M_\bullet}{33 M_\odot} \frac{Z_{\text{nozz}}}{10 R_g} \right)^{0.11 \cdot \chi_2}, \quad (17)
 \end{aligned}$$

with the correction factors

$$\chi_0 = 4.01 - 5.65 i + 3.40 i^2 - 0.76 i^3 \quad (18)$$

$$\chi_1 = 1.16 - 0.34 i + 0.24 i^2 - 0.059 i^3 \quad (19)$$

$$\chi_2 = -0.238 + 2.63 i - 1.85 i^2 + 0.459 i^3, \quad (20)$$

³To simplify the equations we have defined $\gamma_e = \gamma_{e,0} \left(\frac{Q_{\text{jet}}}{10^{39} \text{ erg/sec}} \right)^{0.09}$

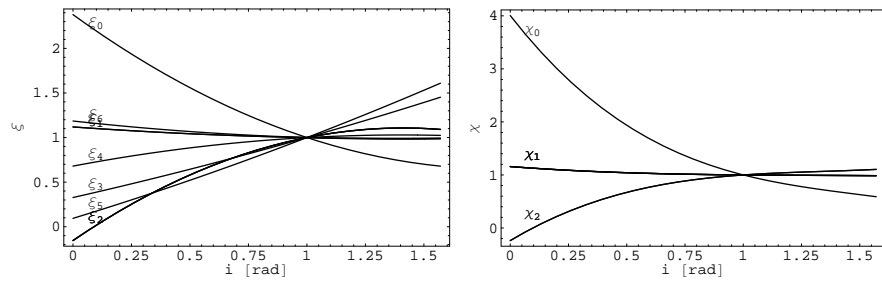


Figure 3: Correction factors ξ and χ for the exponents and factors in Eqs. 9 & 17 as a function of inclination angle i in radians, where $i = 0$ corresponds to face-on orientation. Note, however, that for $i \lesssim 10^\circ$ most approximations fail.

where again the inclination angle i is in radians. We point out that in this model the characteristic size scale of the core region is actually equivalent to the offset of the radio core from the black hole. This does not exclude the existence of emission in components further down the jet, which might be caused by shocks or other processes.

For determining Q_{jet} from the jet model, the flux and to some degree the inclination angle (especially for small i) are most important, while γ_e is mainly determined by the size of the core. Consequently, the latter seems to be the most uncertain part since it is often ambiguous how to define the core and its characteristic size. For practical purposes we can therefore give a yet more simplified formula where we fix γ_e at an intermediate value of 300 and which can be used to very roughly estimate the jet power of a LLAGN from its flux and presumed inclination angle alone (all ξ_n are unity at $i = 1$ rad):

$$Q_{\text{jet}} = 10^{37.6} \text{ erg/sec} \frac{0.024^{\frac{\xi_0}{\xi_1}} 1.56^{\frac{\xi_4}{\xi_1}}}{0.024 \cdot 1.56} \frac{\left(\frac{D}{10 \text{ kpc}}\right)^{\frac{1.6}{\xi_1}} \left(\frac{S_\nu}{\text{mJy}}\right)^{\frac{0.79}{\xi_1}}}{\left(\frac{M_\bullet}{33 M_\odot}\right)^{\frac{0.15 \xi_2}{\xi_1}} \left(\frac{\nu}{8.5 \text{ GHz}}\right)^{\frac{0.15 \xi_2}{\xi_1}} \xi_3^{\frac{0.79}{\xi_1}}} \quad (21)$$

2.4 Application to Famous Sources

One can apply the previously derived relations to various sources and try to explain their radio core properties and derive their basic parameters such as the jet power. This was done for example in Falcke & Biermann (1999) as summarized here in Table 1. The main result is that in three very different, well-observed sources, with very different sizes and fluxes, we can explain the central core with a single model by just scaling the jet power with the accretion rate. The high minimum jet power found for the radio cores justifies in hindsight the assumptions made in earlier papers that jet and disk can be considered symbiotic systems and that – at least in a few systems – the assumption of $Q_{\text{jet}}/L_{\text{disk}} \sim 1$ (or even larger) seems appropriate. This also strengthens the picture that the jets are produced in the inner region of an

Table 1. PARAMETERS OF WELL-STUDIED JET-DISK SOURCES

Source	D	i	ν_{obs} [GHz]	S_ν [mJy]	size [mas]	M_\bullet [M_\odot]	L_{disk} [erg/sec]	Q_{jet} [erg/sec]	$\lg \gamma_e$
GRS 1915+105	12 kpc	70°	15	40	2	(33)	10^{39}	$10^{39.1}$	2.6
NGC 4258*	7.3 Mpc	82°	22	3	0.4	$4 \cdot 10^7$	(10^{42})	$10^{41.7}$	2.8
M81*	3.3 Mpc	35°	8.5	100	0.5	(10^6)	$10^{41.5}$	$10^{41.8}$	2.4

Parameters for compact radio cores in three famous sources. Columns 2-7 are observationally determined input parameters: distance D , inclination angle i of disk axis and jet to the line of sight, observing frequency ν_{obs} , flux density of radio core S_ν , size of radio core, and black hole mass M_\bullet . The inferred disk luminosity L_{disk} is not an input parameter here and given in column 8 for comparison only. Uncertain values are given in brackets, but since the black hole masses do not enter strongly the uncertainties in the black hole mass for M81 and GRS 1915 are actually irrelevant. Columns 9-10 are output parameters of the radio core model: jet power Q_{jet} and characteristic electron Lorentz factor γ_e .

accretion disk, where a major fraction of the dissipated energy is channeled into the jet (Falcke & Biermann 1995; Donea & Biermann 1996).

Another consequence from those radio cores is their amazing scale invariance. It seems that we can use the very same model for a stellar mass black hole which is accreting near its Eddington limit (GRS 1915+105) as well as for a supermassive black hole which is presumably accreting at an extreme sub-Eddington rate (M81, NGC 4258). Moreover, a very similar model works successfully for the quasar sample discussed in the previous section, i.e. supermassive black holes near the Eddington limit. This would suggest that certain properties of an accretion disk/flow, namely jet production, is very insensitive towards changes in accretion rate or black hole mass, and that the 'common engine' mechanism of black hole accretion and jet formation, suggested by Rawlings & Saunders (1991), may include a much larger range of AGN than only quasars and radio galaxies. To check this model we will concentrate in the next section on the central black hole of the Milky Way.

3 The Galactic Center – Sgr A*

The least luminous AGN we can observe is the center of our own galaxy. The ever increasing amount of detailed observations severely constrain any accretion models and give crucial informations for the nature of nuclear radio cores. We therefore should have an in-depth look at Sgr A*, which is the unique 1 Jy flat spectrum radio point source located at the center of the

Galaxy (a more detailed review can be found in Melia & Falcke 2001). Within the Sgr A complex (see Mezger, Duschl, & Zylka 1996 for a review) it is surrounded by a thermal radio source Sgr A West and embedded in the non-thermal “hypernova” shell Sgr A East. Due to its unusual appearance it has long been speculated that this source is powered by a supermassive black hole. Its mass was believed to be around $M_{\bullet} \sim 2 \cdot 10^6 M_{\odot}$ (e.g., Genzel & Townes 1987). In recent years high-resolution imaging (Eckart et al. 1993) and spectroscopy (Haller et al. 1996) in the near-infrared (NIR) have made this case much stronger and the detection of proper motions of stars around the Galactic Center has solidified this case even further (Eckart & Genzel 1996; Ghez et al. 1998) yielding an enclosed mass of $3 \cdot 10^6 M_{\odot}$. The latest development in this direction is that first signs of acceleration in the star’s motion have been found and that the determination of entire orbits will be possible soon (Ghez et al. 2000). This will make the mass determination yet more precise. Moreover, since the relative position of the radio source Sgr A* in the NIR frame has been well determined (Menten et al. 1997) one can also now state that Sgr A* is in the dynamical center of the central star cluster of the Galaxy within $0''.1$ (Ghez et al. 1998). The constraints from the first accelerations found in the stellar proper motions mentioned above seem to have pushed this limit even further, indicating that the center of mass is within 50 milli-arcsecond of Sgr A*. Corroborating evidence that this radio source is associated with the large amount of dark matter comes from the fact that, in great contrast to the surrounding stars, Sgr A* does not show any random proper motion down to a limit of 20 km/sec (Reid et al. 1999; Backer & Sramek 1999), while it does show the apparent linear motion on the sky expected from the sun’s rotation around the Galactic Center. The lower limit placed on the mass of Sgr A* from these observations is around $1000 M_{\odot}$ – much larger than any stellar object or remnant we know of in the Galaxy.

The enormous increase in observational data obtained for Sgr A* in recent years has enabled us to develop, compare, and constrain a variety of models for the emission characteristics of this source. Because of its relative proximity and further observational input to come Sgr A* may therefore become one of the best laboratories for studying supermassive black hole candidates and basic AGN physics at the lowest powers. Hence it is worth to dedicate a separate section to this radio source and briefly summarize what its radio properties are and how we can model its emission.

3.1 The Size of Sgr A*

A problem in determining the size of Sgr A* is that its true structure is washed out by scattering in the interstellar medium (Davies, Walsh, & Booth 1976; van Langevelde et al. 1992; Yusef-Zadeh et al. 1994; Lo et al. 1998) leading to a λ^2 dependence of the apparent size of Sgr A* as a function of observed wavelength. Nevertheless, the mm-to-submm size of Sgr A* is constrained at least within one order of magnitude. From the absence of refractive scintillation Gwinn et al. (1991) have argued that Sgr A* must be

larger than 10^{12} cm at $\lambda 1.3$ and $\lambda 0.8$ mm. Krichbaum et al. (1993) obtained a source size for Sgr A* of $9.5 \cdot 10^{13}$ cm at 43 GHz with VLBI – well above the expected scattering size as extrapolated from lower frequencies. This claim was challenged by Rogers et al. (1994) who only got $2 \cdot 10^{13}$ cm at 86 GHz consistent with the scattering size. Krichbaum et al. (1993) also found an additional weak component and a somewhat elongated source structure at 43 GHz not seen by Backer et al. (1993). The problems of interpreting elongated source structures in Sgr A* with insufficient baseline coverage was discussed recently by Doeleman et al. (1999). The most recent results are by Bower & Backer (1998) who find a source size of $6 \cdot 10^{13}$ cm at 43 GHz ($\lambda 7$ mm) – a mere 2σ above the scattering size, while Lo et al. (1998) infer an elongated source in North-South direction with a size of $5.6 \cdot 1.5 \cdot 10^{13}$ cm. The latter result is a 4σ deviation from the scattering size and would either confirm the basic results of Krichbaum et al. (1993) of a jet-like structure or suffer the same problems as the earlier observations. Finally, observations at 86 ($\lambda 3$ mm) and 215 GHz ($\lambda 1.4$ mm) by Krichbaum et al. (1998) and Doeleman et al. (2001) demonstrate that Sgr A* is compact at a scale around some 10^{13} cm at the highest frequencies, i.e. some 11 Schwarzschild radii for a $3 \cdot 10^6 M_{\odot}$ black hole. While the exact size of Sgr A* cannot yet be stated with absolute certainty, the latest observations fuel hopes that somewhere in the millimeter wave regime the intrinsic source size will finally dominate over interstellar broadening.

3.2 The Spectrum of Sgr A*

There is also some confusion in the current literature about the actual spectrum of Sgr A*. Duschl & Lesch (1994) compiled an average spectrum from the literature and claimed a $\nu^{1/3}$ spectrum indicative of optically thin emission from mono-energetic electrons. However, in early simultaneous multi-frequency VLA observations (Wright & Backer 1993) the actual spectrum was bumpy and the spectral index varied between $\alpha = 0.19 - 0.34$ ($S_{\nu} \propto \nu^{\alpha}$). Morris & Serabyn (1996) published a more recent spectrum that was a smooth power law with $\alpha = 0.25$ below 100 GHz. At low frequencies there is a possible turnover at or below 1 GHz (Davies, Walsh, & Booth 1976).

Of greatest interest for the future debate is the suggestion of a sub-millimeter (submm) bump in the spectrum (Zylka, Mezger, & Lesch 1992; Zylka et al. 1995), since in all models the highest frequencies correspond to the smallest spatial scales. Simultaneous flux density measurement indeed seem to confirm this excess (Fig. 4; Falcke et al. 1998). In the case of Sgr A* one expects the sub-millimeter emission to come directly from the vicinity of the black hole (Falcke 1996).

The submm-bump causing this excess is, in fact, very well explained by assuming the presence of a compact, self-absorbed synchrotron component in Sgr A*. As outlined in Falcke (1996b; see also Beckert & Duschl 1997) this submm component can be described in its most simple minded form by four parameters: magnetic field B , electron density n_e , electron Lorentz

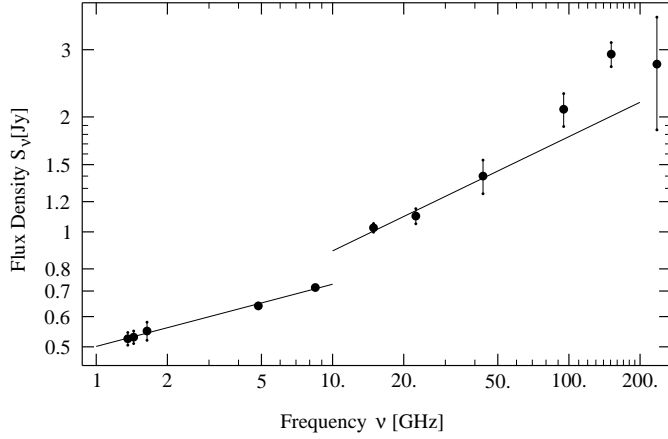


Figure 4: Quasi-simultaneous spectrum of Sgr A* plotted as the logarithm of the flux density vs. the logarithm of the frequency. Shown are the data averaged over the campaign period; flux densities at neighboring frequencies were also combined from the different mm-telescopes. Solid lines represent power law fits to the low- and high-frequency VLA data.

factor γ_e , and volume $V = \frac{4}{3}\pi R^3$, using for simplicity a one-temperature (i.e. quasi mono-energetic) electron distribution and the distance being set to 8.5 kpc. On the other side we have three measurable input parameters: the peak frequency $\nu_{\max} \sim \nu_c/3.5$ of a mono-energetic (or Maxwellian) synchrotron spectrum (characteristic frequency ν_c), the peak flux $S_{\nu_{\max}}$, and the synchrotron self-absorption frequency ν_{ssa} . A fourth parameter can be gained if one assumes that magnetic field and relativistic electrons are in equipartition, i.e. $B^2/8\pi = k^{-1}n_e\gamma_e m_e c^2$ with $k \sim 1$. With this condition we obtain (averaged over pitch angle) that

$$\gamma_e = 118 k^{2/7} \left(\frac{\nu_{\max}}{\text{THz}}\right)^{5/17} \left(\frac{\nu_{\text{ssa}}}{100\text{GHz}}\right)^{-5/17} \left(\frac{F_{\nu_{\max}}}{3.5\text{Jy}}\right)^{1/17}, \quad (22)$$

$$B = 75 \text{ G } k^{-4/17} \left(\frac{\nu_{\max}}{\text{THz}}\right)^{7/17} \left(\frac{\nu_{\text{ssa}}}{100\text{GHz}}\right)^{10/17} \left(\frac{F_{\nu_{\max}}}{3.5\text{Jy}}\right)^{-2/17}, \quad (23)$$

$$n_e = 2 \cdot 10^6 \text{ cm}^3 k^{7/17} \left(\frac{\nu_{\max}}{\text{THz}}\right)^{9/17} \left(\frac{\nu_{\text{ssa}}}{100\text{GHz}}\right)^{25/17} \left(\frac{F_{\nu_{\max}}}{3.5\text{Jy}}\right)^{5/17}, \quad (24)$$

$$R = 1.5 \cdot 10^{12} \text{ cm } k^{-1/17} \left(\frac{\nu_{\max}}{\text{THz}}\right)^{-16/51} \left(\frac{\nu_{\text{ssa}}}{100\text{GHz}}\right)^{-35/51} \left(\frac{F_{\nu_{\max}}}{3.5\text{Jy}}\right)^{8/17} \quad (25)$$

Apparently the ‘non’-equipartition parameter k enters only weakly and as long as one is not many orders of magnitude away from equipartition the

parameters are basically fixed within a factor of a few and we can make solid arguments about the possible source size of Sgr A* at submm wavelengths. As VLBI measurements are only available at longer wavelengths one could still postulate arbitrarily large submm source sizes. However, if Sgr A*(submm) were optically thin and larger than $4 \cdot 10^{13}$ cm we should have seen the low frequency $\nu^{1/3}$ part of its spectrum with 3mm VLBI already. This could only be avoided if the submm component becomes optically thick below ~ 100 GHz. As shown above this is possible only for a very compact source where the dimensions of Sgr A* at submm wavelengths are substantially *smaller* than at $\lambda 3$ mm. Consequently Sgr A* has to be of the same size or smaller at submm wavelengths than at $\lambda 3$ mm.

This size is consistent with the upper limits (~ 1 AU) from VLBI and lower limits ($\sim 10^{12}$ cm) from scintillation experiments as discussed above. In comparison we also note that the Schwarzschild radius (R_S) of the putative $3 \cdot 10^6 M_\odot$ black hole in the Galactic Center is already $R_S = 0.9 \cdot 10^{12}$ cm and thus the compact submm component should correspond to a region in the very vicinity of the black hole. Most interesting is the possibility that this region is directly affected by general relativistic effects, and could for example be gravitationally amplified if the radiation is intrinsically anisotropic (e.g., similar to Cunningham 1975). Finally, such a compact component with the parameters as in Eq. 25 would be very interesting for mm-VLBI, since the black hole horizon could be imaged against the background of this submm emission. This will be discussed in greater detail below (Sec. 3.5).

Finally, as an important new window to Sgr A*, one needs to mention that interesting new information on the polarization properties of Sgr A* is available. In short one can say that Sgr A* stands out by having relatively strong circular polarization but no detectable linear polarization (Bower et al. 1999a; Bower, Falcke, & Backer 1999) below 43 GHz – the situation at higher frequencies is still a bit unclear (Bower et al. 1999b; Aitken et al. 2000). Since there is not enough space to discuss here the relevance of this finding, one should just point out that this probably requires the presence of rather cold ($T_e \sim 10^9$ K) electrons in addition to the hot electrons required for producing the submm-bump ($T_e \sim 10^{11}$ K, Beckert et al., in prep.)

3.3 Accretion Models – An Overview

If we now want to go beyond a mere description of Sgr A*, we have to ask how this source is powered and what the underlying engine producing the radio and X-ray emission actually is? One idea is that, if Sgr A* is a black hole, it should swallow some fraction of the strong stellar winds seen in the Galactic Center through spherical (Bondi-Hoyle) accretion.

The rate of infall depends only on the mass of the black hole and the wind parameters. The general validity of the Bondi-Hoyle accretion (without angular momentum) under these assumptions was demonstrated by 3D numerical calculations (Ruffert & Melia 1994) and the main uncertainties are related to the plasma physical effects associated with the infall. It is usually assumed

that the magnetic field in the accreted plasma is amplified by compression up to a point where it reaches the equipartition value. Beyond this point the excess magnetic field is assumed to be dissipated and used to heat the plasma. The electron temperature is determined by the equilibrium between heating and cooling via cyclo-synchrotron radiation where one has to consider two domains for the solution of this problem: (1) hot electrons, where the typical electron Lorentz factors are of the order 100-1000 and (2) warm electrons, where the electron Lorentz factor is still close to unity.

The first domain is in a regime where synchrotron emission is important and also very effective. This requires only low accretion rates ($\dot{M} \sim 10^{-10} M_{\odot}/\text{yr}$) which seems to be in contradiction with the naive expectations of the Bondi-Hoyle accretion rate for a $3 \cdot 10^6 M_{\odot}$ black hole (Ozernoy 1992; Mastichiadis & Ozernoy 1992)⁴. The radio spectrum in such a configuration is mainly due to the optically thin part of a quasi mono-energetic (or Maxwellian) electron distribution and was calculated also by Duschl & Lesch (1994), Beckert & Duschl (1997), and to some degree also used within the jet model (Falcke 1996, but optically thick).

The second domain is in the transition regime between cyclotron and synchrotron radiation, which is less effective than pure synchrotron radiation and hence requires higher accretion rates ($\dot{M} \sim 10^{-4} M_{\odot}/\text{yr}$; Melia, Jokipii, & Narayanan 1992; Melia 1992; Melia 1994) but also over-produces thermal X-rays (see below).

The big advantage of the wind-accretion approach would be that it, firstly, appears unavoidable and, secondly, self-consistently ties observable parameters and accretion rate to the mass of the central object.

On the other hand there are several problems to be considered: firstly, it is not at all clear that the wind-producing stars, as an ensemble, have zero angular momentum, thus producing a non-zero angular momentum of the winds to be accreted. This would diminish the accretion rate. Hydrodynamical simulations show that the exact distribution and velocity of stellar wind sources within the observationally allowed range indeed can change the expected accretion rate (Coker & Melia 1997). Another question is whether the stellar winds are indeed isotropic. The only resolved stellar wind seen in the Galactic Center so far, the wind of IRS 7 (Yusef-Zadeh & Morris 1991), looks like a cometary tail pointing *away* from Sgr A*. This raises the question whether there is a wind (Chevalier 1992) or expanding bubble pushing gas *out* of the Galactic Center.

There also could be residual angular momentum in Sgr A* itself, e.g., because of a fossil accretion disk which could catch the inflow further out, filling a reservoir of rather dense matter instead of directly feeding the black hole. The viscous time scales of such a disk can be very long – up to 10^7 years (Falcke & Heinrich 1994). However, detailed calculations of such a process (Falcke & Melia 1997; Coker, Melia, & Falcke 1999) indicate that the impact

⁴These authors turned the argument around and used the reduced accretion rate to argue for a lower mass black hole, something that seems to be excluded by now

of the wind onto the fossil disk should produce a non-negligible IR emission that is not seen.

An alternative to the models mentioned above was proposed by Narayan, Yi, & Mahadevan (1995) and Narayan et al. (1998), who explain the discrepancy between high accretion rate and low luminosity by the effects of an advection dominated accretion flow (ADAF) or disk. In this model more than 99.9% of the energy is not radiated but transported through the disk by advection and finally swallowed by the black hole. And, in fact, it appears as if advection is non-negligible in many accretion disks, but whether indeed such a high fraction of the energy is transported by advection alone is not at all clear. One also has to make sure that not a substantial fraction of the energy is released in the inner parts of the disk and that the energy is swallowed quietly by the black hole⁵. Even if an advection dominated accretion flow is not the whole story, it may be an interesting part of it.

A major problem of the ADAF model is that it under-predicts the cm-wave emission in the spectrum of Sgr A* by more than an order of magnitude. In Narayan et al. (1998) this is fixed by artificially assuming a constant electron temperature in the accretion flow over a particular range in radius r . The range was hand-picked such that the cm-wave spectrum is fitted by a $\nu^{1/3}$ spectrum, reminiscent of the spectra produced by Ozeroy (1992) and Beckert & Duschl (1997). Another fix was proposed by Mahadevan (1998) who added a power-law distribution of protons producing high-energy pairs in hadronic interactions. The proton power law would require shock acceleration in the accretion flow which requires turbulent plasma waves (e.g., Schlickeiser, Campeanu, & Lerche 1993; Schneider 1993). It has to be ensured that these waves do not couple to electrons as well, otherwise this would lead to heating and shock acceleration of electrons. In this case the basic assumption of a two-temperature plasma, a fundamental assumption of ADAFs, would break down.

The latest information for Sgr A* comes from the possible detection of Sgr A* at X-ray wavelengths with the satellite Chandra (Baganoff et al. 2001). The first epoch data show a point source at the location of Sgr A* with a rather low X-ray luminosity around $0.5 - 1 \cdot 10^{34}$ erg s⁻¹ in the 0.5-10 keV band (Baganoff et al., priv. comm.) – even lower than the earlier ROSAT results (Predehl & Trümper 1994). This new measurement provides a crucial constraint for any model of radiative emission from Sgr A* since the spectral index is apparently rather steep with a photon index around 2.6 (Baganoff, priv. comm.). This seems to rule out free-free emission from hot electrons as expected in Bondi-Hoyle or ADAF models and requires those models to significantly lower their accretion rate.

⁵But again, X-rays become more and more of a problem.

3.4 The Jet Model for Sgr A*

In the following we will now concentrate on the jet model for Sgr A* which allows one to self-consistently explain radio and X-ray emission using the model outlined before. A more detailed description is given in Falcke & Markoff (2000).

Given an initial magnetic field B_0 , a relativistic electron total number density n_0 with a characteristic electron energy $\gamma_{e,0}m_e c^2$, radius r_0 of the nozzle, and taking only adiabatic cooling due to the longitudinal pressure gradient (i.e. $\propto \mathcal{M}^{\Gamma-1}$, where \mathcal{M} is the Mach number) and dilution by the lateral expansion into account, one can determine the magnetic field $B(z)$, particle density $n(z)$, electron Lorentz factor $\gamma_{e,0}(z)$, and jet radius as a function of the distance from the nozzle and then calculate the spectrum of the jet in a straight forward way.

The basic parameters for the jet – B_0 , $\gamma_{e,0}$, and r_0 – are fixed within a factor of a few by the location of the submm-bump in the spectrum and which, in this model, is mainly produced by emission from the nozzle (Falcke 1996). The steep cut-off in the Sgr A* spectrum towards the IR further constrains the electron distribution. It indicates the lack of a power-law tail of high-energy electrons, which usually produces the optically thin high-frequency emission seen, for example, in Blazars.

Figure 5 shows a fit to the submm and cm radio spectrum with the nozzle parameters given in the plot. We are plotting F_ν rather than νF_ν thus allowing one to better judge the quality of the spectral fit at cm-waves. The nozzle component accounts for most of the submm-bump, as well as the main Compton component reproducing the X-ray emission, and the low-frequency radio spectrum stems from the emission of the more distant parts along the jet. Within the model, the slope of the cm-wave spectrum and the ratio between cm and submm emission is mainly determined by the inclination angle. The parameters we obtain for jet and nozzle are very close to those used by Falcke (1996), Beckert & Duschl (1997), and Falcke & Biermann (1999). The jet-specific parameters appear reasonable: the inclination angle is rather average, size of the nozzle is a few times R_s , and the system is very close to equipartition.

Since the X-ray emission is thought to be up-scattered submm-wave emission, the predictions from this model are clear: we would expect significant SSC emission in the softer X-ray band. Given the variability of the radio emission we also expect to see correlated submm and X-ray variability. Complete absence of X-ray variability would argue against SSC emission giving a major contribution.

3.4.1 VLBI Size and Extended Emission

Possibly the most important constraints for any model are the VLBI measurements of the size of Sgr A*. Since most models have a stratified structure, the size of Sgr A* is expected to be a function of frequency. We note that for a

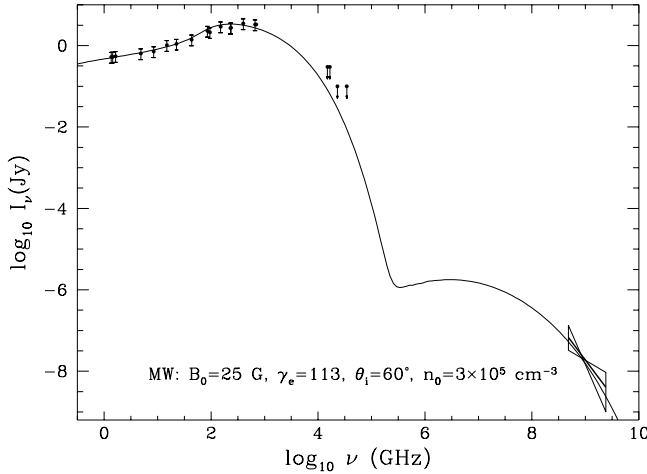


Figure 5: Broad-band spectrum of Sgr A* for a relativistic Maxwellian distribution of relativistic electrons in a jet. The width of the nozzle is $r_0 = 4R_s$ and $r_0 = 3R_s$ respectively, while its height is $z_0 = 3r_0$. The dots are the simultaneous spectrum measured by Falcke et al. (1998) with additional high-frequency data from Serabyn et al. (1997). In the hard X-rays we show the possible detection of Sgr A* with Chandra (Baganoff et al. 2001).

given observing frequency the emission in the jet model is highly concentrated to one spatial scale. The emission from the jet at a particular frequency is self-absorbed at small distances from the origin and cuts off at large distances where the decreased magnetic field shifts the synchrotron cut-off frequency below the observing frequency. This is illustrated in Fig. 6, where we show a longitudinal cut through the jet based on our model. Each line corresponds to a different observing frequency and one can see that the flux towards larger distances from the core falls off rather steeply, i.e. exponentially rather than with a power law.

Thus, extended emission from the jet is highly (almost exponentially) suppressed and the size of the detectable core will be a power law $z \propto \nu^{-\aleph}$ with \aleph in the range 0.9 to 1. This also implies a shift of the location of the core with frequency. Figure 7 compares the predicted full width at half maximum (FWHM) of major and minor axis of the emission predicted by the jet model with the constraints imposed by high-frequency VLBI observations. Throughout the cm-wave range the emission basically resembles one elliptical component decreasing in size with wavelength and only at mm-waves (i.e. above 30 GHz) an even more compact core-component, the nozzle, appears. Hence, as long as the FWHM predicted in the model is compatible with the observed values it will be difficult to distinguish the Sgr A* source structure at one frequency from a Gaussian VLBI component.

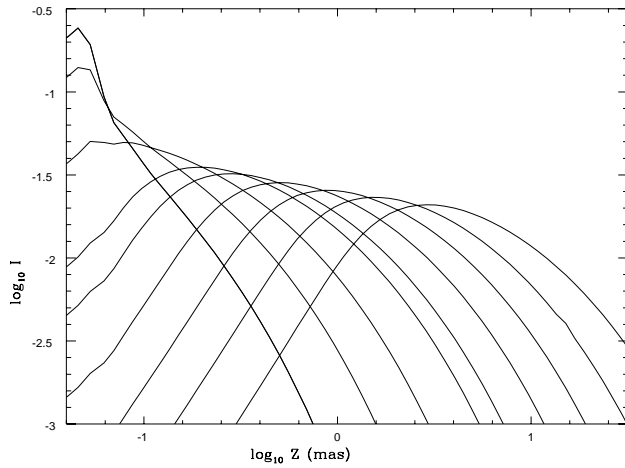


Figure 6: Longitudinal cuts along the jet axis for our model (Maxwellian electron distribution) at various frequencies (220, 90, 43, 21, 15, 8.5, 4.8, 2.7, & 1.4 GHz). Plotted are the observed flux per segment in arbitrary units versus the observed separation in milli-arcseconds (mas) from the black hole. Curves to the left represent higher frequencies and the spikes in the left-most flux distributions are due to the nozzle.

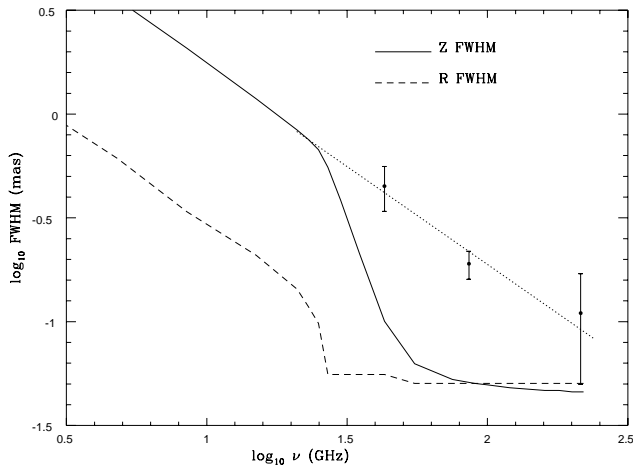


Figure 7: FWHM of the major and minor axis of the jet model as a function of frequency. The filled dots mark the FWHM as measured by Lo et al. (1998; 43 GHz) and Krichbaum et al. (1998; 86 & 215 GHz). At frequencies above 30 GHz one obtains a two component structure with an increasingly stronger core (nozzle, solid dashed line) and a fainter jet component (dotted line). This structure will be largely washed out by interstellar scattering.

3.4.2 Conclusions from Applying the Jet Model

The spectrum of Sgr A*, including the new X-ray observations from Chandra, can be modeled entirely by emission from this jet alone. We can also show that the radio emission satisfies all constraints imposed by VLBI observations. This shows that the basic model introduced by Falcke, Mannheim, & Biermann (1993) can provide a detailed explanation of the Sgr A* radio and X-ray spectrum. It also fits Sgr A* within the frame work of compact radio cores discussed in Sections 2 and 4.

One counter argument often heard in the context of modeling Sgr A* as a jet is that one does not see a jet. However, in typical AGN core-jet sources the extended jet structure is due to emission from an optically thin power law. Here this extended emission is greatly suppressed due to the steep cut-off in the electron spectrum, required by the IR limits. This naturally can explain the compact (jet?) structure as seen by Lo et al. (1998) and Doeleman et al. (2001). Sgr A*, basically is a naked core without much extended jet emission. The lack of optically thin emission could also help to reduce the level of linear polarization in Sgr A* compared to more powerful AGN (Bower et al. 1999a; Bower, Falcke, & Backer 1999; Bower et al. 1999b) since the degree of polarization decreases to zero near the self-absorption frequency due to radiation transfer effects.

The main assumption of the model is the presence of a nozzle close to the central black hole collimating a relativistic plasma with approximate equipartition between the magnetic field and relativistic particles. The evolution of magnetic field and particle density is calculated self-consistently and does not require additional parameters beyond those fixed for the nozzle. The spectra we obtain are therefore generic for collimated outflows from any accretion flow – whether a magneto-hydrodynamical jet from a standard accretion disk or an outflow from an ADAF – provided the accretion flow can produce the required magnetic field, electron temperature, and density near its inner edge. For an ADAF or Bondi-Hoyle type accretion the presence of a jet near the black hole could thus aid those models in accounting for the cm-wave radio emission, which is especially difficult. The energy requirements to produce such a jet (see Falcke & Biermann 1999) are rather small compared to the power available through accretion of nearby winds (Coker & Melia 1997).

It remains to be seen whether one can construct a self-consistent model which couples an outflow as described here together with, for example, an ADAF model (Yuan 2000). Particularly interesting in this context is whether one could reproduce the unusual electron distribution found in Sgr A*. As pointed out in Falcke (1996) the typical electron Lorentz factors required in the nozzle are close to those expected from pair production in proton-proton (pp) collisions. Mahadevan (1998) showed that an ADAF could in principle provide the environment where pp-collisions could play an important role even though in this paper a power-law distribution of protons had to be artificially added. More detailed calculations in this direction are being undertaken (Markoff et al., in prep.).

3.5 Future Prospects - Imaging of the Event Horizon

The existence of a very compact nozzle radiating at mm- and submm-wavelengths is intriguing since the size of Sgr A* could be less than 15 Schwarzschild radii (0.11 mas at 215 GHz) for a black hole mass of $3 \cdot 10^6 M_\odot$ at a distance of 8 kpc. Of all the known black hole candidates, Sgr A* is the source where the angular size on the sky of its Schwarzschild radius is the largest. In fact, the angular resolution of ground-based VLBI experiments now comes interestingly close to the scale where significant general relativistic effects are important.

We have considered an optically thin emission region with frequency-independent emissivity around a black hole with arbitrary spin (Falcke, Melia, & Agol 2000b; Falcke, Melia, & Agol 2000a). The intensity and structure of the emission region can be arbitrary as well, but we choose a number of generic scenarios where we have either a spherical distribution of the intensity scaling as a power-law with radius r or a jet-like distribution (hollow cylinder). We also can allow for various velocity fields, e.g., with rotation, inflow, or outflow. The appearance of the emission region for an observer at infinity, taking all general relativistic effects into account, is then calculated using a standard formalism (e.g., Thorne 1981; Viergutz 1993; Jaroszynski & Kurpiewski 1997).

To test whether general relativistic effects would be visible we convolved the resulting images from the ray-tracing calculations with two Gaussian beams: one representing the scatter-broadening of the image due to the interstellar material along our line-of-sight towards the Galactic Center and one representing the finite resolution of VLBI with 8000 kilometer baselines. The width of the former has a ν^{-2} (e.g., Lo et al. 1998) and the latter a ν^{-1} dependence.

Regardless of the exact emission model we use, we find a characteristic structure in all models: a bright ring of emission with a pronounced deficit of emission inside of that (Fig. 8). We call the deficit in the inner region the ‘‘shadow’’ of the black hole since it is caused by the deficit of photons emitted near the black hole that have disappeared into the event horizon or are bent away from our line of sight. The circumference of the shadow is determined by the ‘‘photon-orbit’’—a theoretical orbit where photons can circle the black hole an infinite number of times, but when perturbed may escape to infinity

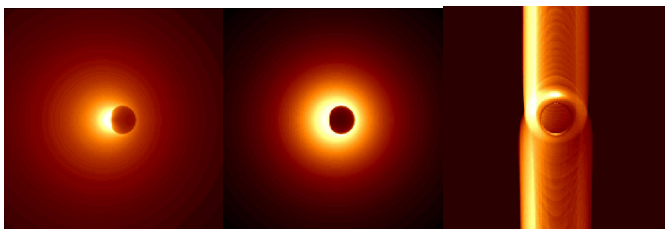


Figure 8: Images of the shadow of a black hole for rotating and non-rotating black holes and for spherical and jet-like emission models.

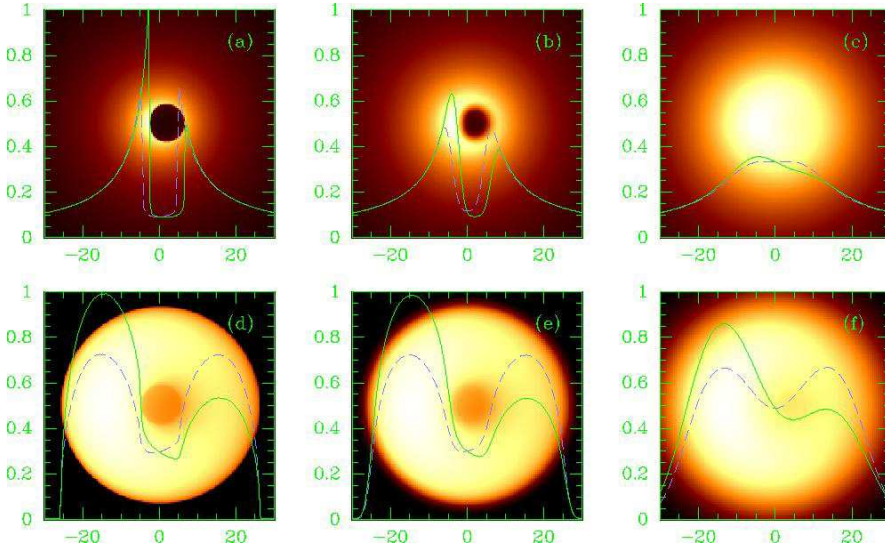


Figure 9: The expected shadow of Sgr A*. a) the ray-tracing simulation; b) simulated VLBI image at $\lambda 0.6\text{mm}$; c) simulated VLBI image at $\lambda 1.3\text{mm}$ (see Falcke et al. 2000 for details).

(Bardeen 1973). Interestingly, the size of this shadow is much larger than the event horizon—due to gravitational lensing—and is always of the order $10 R_g$ ($R_g = GM_\bullet/c^2$) for rotating and non-rotating black holes.

The exact intensity distribution of the bright ring depends significantly on the nature of the emission region, however. A rotating inflow would produce a slightly asymmetric ring due to Doppler boosting of one side of the shells in Keplerian rotation. A jet would look even more asymmetric since boosting due to rotation plus fast outflow would enhance one quadrant of the ring (Fig. 8).

The relatively large size of the shadow is of particular interest for Sgr A*, since at a wavelength of around 1.3 mm the black hole shadow, the scattering disk, and the possible resolution of mm-VLBI become comparable. This is illustrated in Figure 9. It is clear that at wavelengths shortwards of $\lambda 1.3$ mm the shadow could actually be imaged with ground-based telescopes.

The possibility of seeing the effect of an event horizon is tantalizing. The shadow of the black hole in the Galactic Center is expected to have a diameter of $\sim 30 \mu\text{as}$. The highest resolution so far achieved with VLBI is $\sim 50 \mu\text{as}$. To achieve the additional improvement of a factor of two to three in resolution would require extending mm-VLBI to submm wavelengths. While this is difficult because of atmospheric effects, it is not technically impossible. Quite a number of submm-telescopes and arrays are currently under construction or consideration that could be used for such an experiment.

Another concern is whether the source itself could become an obstacle. Clumpiness of the emission may not be a major source of confusion because

of the short rotation timescale of about 100 seconds. Optical depth effects could be a major problem. However, currently available submm spectra of Sgr A* indicate a rather flat spectrum with a turnover towards the infrared. Hence at some wavelength between mm-radio and IR the source is bound to be optically thin. A second pitfall is anisotropic beaming. In the jet model, for example, one quadrant is amplified due to relativistic beaming, making it more difficult to pick out the entire faint ring with low resolution or low dynamic range observations.

Without a better understanding of spectrum, structure, and nature of the emission it will be difficult to predict exactly at what wavelength the shadow will be unambiguously detectable and how much technical development still has to be done. In any case there is no reason to think that imaging the shadow is in principal impossible and any upcoming VLBI experiment at 1.3 mm and shorter wavelengths involving Sgr A* from now on could already show the first signs of the event horizon.

4 Low-Luminosity AGN

In Section 2 we have discussed the general theory of compact radio cores and the jet-disk symbiosis which was then applied to Sgr A*. The conclusion was that compact radio cores are rather scale invariant and only subject to changes in the accretion rate onto the central black hole. With the finding of black holes in many nearby galaxies and the identification of a huge crowd of low-luminosity AGN, many of them compiled in the spectroscopic atlas by Ho, Filippenko, & Sargent (1995), it was clear that from this theory one would expect a large number of galaxies with compact radio cores (see also Perez-Fournon & Biermann 1984). These radio cores should bridge the gap between Sgr A* and quasars. The imperative then was to find them in a significant number and compare their properties with more luminous counter parts.

This comparison is also important since the question of how central engines in high and low-luminosity AGN are related to each other and why they appear so different despite being powered by the same type of object is of major interest. For many nearby galaxies with low-luminosity nuclear emission-lines, it is not even clear whether they are indeed powered by an AGN or by star formation – despite many of them being called LLAGN.

Earlier surveys have shown that E and S0 galaxies often have compact, flat-spectrum radio sources in their nuclei (Wrobel & Heeschen 1984; Slee et al. 1994). Some of the most prominent flat-spectrum nuclear radio sources in nearby galaxies are found in galaxies with LINER nuclear spectra (O’Connell & Dressel 1978), but so far there has been no comprehensive study of radio nuclei in a significant sample of LINER galaxies, which make up the majority of galaxies with low-level nuclear activity. We have, therefore, recently conducted a survey of LINER galaxies with the VLA at 15 GHz (resolution $\sim 0''.15$) and the VLBA at 5 GHz (resolution $\sim 0''.002$) to search for compact

radio emission (Nagar et al. 2000; Falcke et al. 2000). In the following sections the results of this search for “siblings of Sgr A*” and their interpretation are presented.

4.1 Detection of Flat-Spectrum Radio Cores with the VLA

Observations were made of two samples (Nagar et al. 2000; Falcke et al. 2000). All sources were drawn from the extensive and sensitive spectroscopic study of the complete, magnitude-limited sample of 486 nearby galaxies mentioned above (Ho, Filippenko, & Sargent 1995), one third of which showed LINER-like activity (Ho, Filippenko, & Sargent 1997). From these active galaxies with a LINER spectrum a subsample (dubbed “48 LINERs” sample) of 48 bright sources was drawn with no well-defined selection criterion other than that they had been observed with other telescopes as well, e.g., ROSAT, the HST (UV imaging, Maoz et al. 1996; Barth et al. 1998), and the VLA at 1.4 and 8.4 GHz in A and B configuration (van Dyk & Ho 1998). The sample also included so-called transition objects which have spectra intermediate between LINER and H II region galaxies. While the project was being conducted a few sources in the original LINER sample were re-classified as low-luminosity Seyfert galaxies. Transition objects were included because for these objects it was not clear whether their emission-line spectrum is produced by intense star formation or whether they are simply LINERs with a very faint AGN.

In a second step we compiled a distance limited sample (dubbed “96 LLAGN” sample) from the (Ho, Filippenko, & Sargent 1995) atlas, selecting all galaxies with LINER, Seyfert, and transition spectra within 19 Mpc. This will reduce the effects of any bias that might have come from the rather ill-defined selection criterion of the first sample. By including LINERs, Seyferts, and Transition objects we will also be able to see possible differences in the detection rates between the different types. By choosing a distance limited sample, constrained to the very local universe, we also make sure to study the faintest AGN we can find today.

Both samples were observed with the VLA at 15 GHz in its largest configuration (A) providing maximal resolution, i.e. up to $0''.15$ corresponding to a linear scale of 14 pc at a distance of 19 Mpc. The 5σ detection limit was around 1 mJy.

The rationale behind going to this setup is that the extended emission from AGN is optically thin and steep-spectrum. Radio cores, on the other hand – if they are produced on scales very close to the AGN – are optically thick, and compact at milli-arcsecond scales. This means that by going to the configuration with the highest resolution one will resolve out most of the extended emission and get a clearer view on the compact structure. At higher frequencies this effect is even stronger since the beam size is inversely proportional to the frequency, reducing the extended flux per beam. The steep spectrum will diminish the flux density of the extended emission even further. The reason that one does not go to even higher frequencies is simply a

technical one, since the achievable sensitivity with the current instrumentation of the VLA becomes increasingly worse at 22 and 43 GHz.

The results of the first survey for the 48 LINERs is that we detected relatively many, namely 18 out of 48 galaxies (37%). Split into the different groups we detected only 1 out of 18 transition objects, but 6 out of 8 Seyferts and 11 out of 22 LINERs, yielding a combined detection rate for Seyferts and LINERs of 57% compared to only 6% for transition objects.

Using literature data (the VLA data at lower frequencies are still being processed by another group) it was possible to determine whether the detected cores should be considered as flat- or steep-spectrum cores. Out of the 18 detected cores only two apparently had a steep radio spectrum. Hence, the 15 GHz VLA observations were indeed properly designed to discriminate against steep-spectrum emission and to pick out the flat-spectrum cores.

The high detection rate is confirmed by observations of the second sample (Falcke et al., in prep.). Since this is a distance limited sample selection effects should be minimized. The detection rate is 32 out of 95 galaxies (one galaxy was lacking data), i.e. 34%. In the sample we detected only 6 out of 38 transition galaxies (16%), while we detected 26 out of 57 Seyferts and LINERs (46%). The large majority of these detections are in fact confirmed as flat-spectrum cores.

We can therefore conclude that galaxies with Seyfert and LINER spectra are much more likely to contain flat-spectrum radio cores than transition objects. The latter are therefore probably significantly weaker AGN or are largely dominated by starbursts. On the other hand, if one considers flat-spectrum cores as evidence for a black hole powered AGN, we can conclude that at least about half of LINERs and Seyferts are indeed genuine AGN. If we can combine both samples we find no significant difference in the detection rates between Seyferts and LINERs.

However, one could still wonder whether the flat-spectrum cores are really AGN related. In principle the flat spectrum could also be produced by a giant free-free emission region in a star forming region. To exclude this possibility one needs to go to even higher resolution and observe the respective galaxies with VLBI. This will allow one to probe brightness temperatures around 10^8 K for the cores of interest here and distinguish between the two cases.

4.2 Detection of Flat-Spectrum Radio Cores with the VLBA

From our 48 LINERs sample (previous section), we selected all eleven galaxies with both nuclear flux densities above 3.5 mJy at 15 GHz and a flat spectrum ($\alpha > -0.5$, $S_\nu \propto \nu^\alpha$). The flux density limit was chosen so that we could detect all sources with the VLBA in snapshot mode in a single 12 hr observation if most of the 15 GHz emission were indeed compact on milli-arcsecond (mas) scales. The observations are more extensively described in Falcke et al.

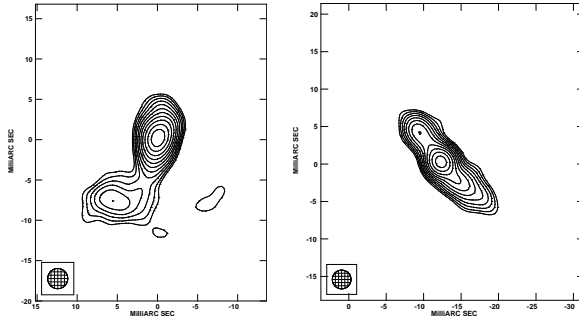


Figure 10: VLBA maps of NGC 4278 (left) and NGC 6500 (right). The beam is 2.5 milli-arcsecond and contours are integer powers of $\sqrt{2}$, multiplied by the $\sim 5\sigma$ noise level of 0.9 mJy. The peak flux densities are 37.3 mJy and 35.8 mJy respectively.

(2000) and indeed all sources were detected with the VLBA⁶.

The two brightest sources in our sample, NGC 4278 & NGC 6500, for which we have the largest dynamic range, show core plus jet structures (Fig. 10). The spectral indices of the whole sample range from $\alpha = -0.5$ to $\alpha = 0.2$, with an average $\langle\alpha\rangle = 0.0 \pm 0.2$. Using our beam size of 2.5 milli-arcsecond and the peak 5 GHz flux densities (Table 1 in Falcke et al. 2000), we find brightness temperatures in the range $T = 0.25 - 2.9 \cdot 10^8$ K for our sample, with an average brightness temperature for all sources of $\langle T_b \rangle = 1.0 \cdot 10^8$ K. Since most of our sources are unresolved, these values are usually lower limits.

Our result has a number of interesting implications. The presence of high brightness temperature radio cores in our LINER sample confirms the presence of AGN-like activity in these galaxies. It is unlikely that the radio sources represent free-free emission, as has been claimed for example in NGC 1068 (Gallimore, Baum, & O’Dea 1997), since a much higher soft X-ray luminosity than is typically observed in low-luminosity AGN would be expected.

On the other hand, the compact, flat-spectrum cores we have found are similar to those typically produced in many AGN. Hence we can take the presence of compact, non-thermal radio emission as good evidence for the presence of an AGN in our galaxies. The 100% detection rate with the VLBA, based on our selection of flat-spectrum cores found in a 15 GHz VLA survey, shows that for statistical purposes we could have relied on the VLA alone for identification of these compact, high brightness radio sources. Hence, with 15 GHz VLA surveys of nearby galaxies one has an efficient tool for identifying low-luminosity AGN. This complements other methods for identifying AGN, such as searching for broad emission-lines or hard X-rays, and has the advantage of not being affected by obscuration.

⁶The one source for which the data reduction had initially failed was detected in a subsequent observing run (Nagar et al., in prep.)

4.3 Radio Cores in LLAGN – the Grand Perspective

Assuming the cores detected in the VLA & VLBA survey are produced by randomly oriented, maximally efficient jets from supermassive black holes (of order $10^8 M_\odot$) we can use Eq. 21 to calculate a minimum *total* jet power. For an average monochromatic luminosity of $10^{27.5}$ erg sec $^{-1}$ Hz $^{-1}$ at 5 GHz the jets would have powers of order $Q_{\text{jet}} \gtrsim 10^{42.5}$ erg sec $^{-1}$. The way the model was constructed one has to consider this a minimum energy estimate. Still, compared to quasars this is a rather low value and supports the conclusion, based on their low UV and emission-line luminosities, that the cores are powered by under-fed black holes. On the other hand this jet power is well within the range of the bolometric luminosity of typical low-luminosity AGN (10^{41-43} erg sec $^{-1}$; Ho 1999) and, compared to radiation, jets should be a significant energy loss channel for the accretion flow.

This similarity between jet power and (accretion) luminosity, of course, appeals again to the jet-disk symbiosis picture discussed at the beginning of this work. We can now take the radio cores detected in our survey and put them on the correlation predicted in Falcke & Biermann (1996). A problem one encounters is how to estimate the accretion disk luminosity and accretion power. To make the different AGN comparable we will use the narrow H α line that is measurable in all AGN, and apply the same conversion factor between H α and L_{disk} as used for quasars. For narrow H α Eq. 6 then reads

$$\lg(L_{\text{disk}}/\text{erg s}^{-1}) = 4.85 + \lg(L_{\text{H}\alpha,\text{n}}/\text{erg s}^{-1}). \quad (26)$$

This estimate of course underestimates the accretion power or accretion rate compared to quasars if LLAGN are largely dominated by inefficient accretion, such as ADAFs. Figure 11 shows the predicted Radio/ L_{disk} correlation together with LLAGN found in our survey. The galaxies almost fill the gap between quasars and X-ray binaries on this absolute scale and roughly fall in the predicted range. This illustrates that we have a continuation from high-luminosity to low-luminosity AGN, *the latter being the silent majority within the AGN family.*

We can investigate the optical/radio correlation in greater detail. For the VLBI-sample (Nagar et al., in prep.), i.e. the well-detected cores above 3 mJy in both samples, for which we have basically established that the radio emission is AGN-related, we can look at correlations between radio, emission-line, and bulge luminosities. Figure 12 (right panel) shows that there is a trend for galaxies with higher H α emission to have more luminous radio cores. Interestingly, elliptical and spiral host galaxies are offset from each other. The same effect can be seen in Fig. 11 where one finds a string of sources connecting to FRI radio galaxies and falling somewhat above the top line predicted by the model. This are the large elliptical galaxies which are probably faint versions of radio galaxies. Does this reflect a radio-loud/radio-quiet dichotomy for LLAGN?

In this respect it is noteworthy that both populations seem to lie somewhat above the expected theoretical radio-optical distribution. The radio cores in

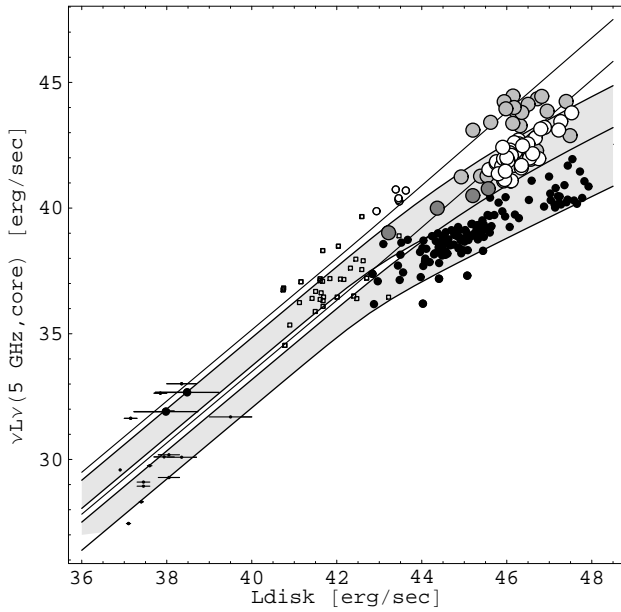


Figure 11: Correlation between thermal emission from the accretion disk (with the exception of X-ray binaries this is basically normalized to the narrow $H\alpha$ emission) and the monochromatic luminosity of black hole radio cores. Open circles: Radio-loud quasars; small open circles: FRI radio galaxies; open gray circles: Blazars and radio-intermediate quasars (dark grey); black dots: radio-quiet quasars and Seyferts; small dots: X-ray binaries; small boxes: detected sources from the “48 LINERs” sample. The latter apparently confirm the basic prediction of Falcke & Biermann (1996) and almost close the gap between very low (on an absolute scale) accretion rate objects and high accretion rate objects. The shaded bands represent the radio-loud and radio-quiet jet models as a function of accretion as shown in Falcke & Biermann (1996).

ellipticals are most likely the continuation of FRI radio galaxies at low powers. For FRI radio galaxies it is known that they seem to be underluminous in emission lines (e.g. Falcke, Gopal-Krishna, & Biermann 1995; Zirbel & Baum 1995). If one would artificially increase L_{disk} by a factor of about 30, the radio cores in ellipticals and FRIs would nicely connect to those of FRII radio galaxies and radio loud quasars. Applying the same factor to the spiral galaxy cores would shift the remaining population into the radio-quiet regime. Such a shift would be appropriate if, for a given accretion rate or jet power, the radiative efficiency of the disk would be reduced by such a factor (e.g. as in some ADAF models).

There is, however, another important factor: the galaxy bulge luminosity. We do see a weak trend for the radio luminosity to be related to bulge luminosity; also the ratio between radio and $H\alpha$ luminosity tends to increase with increasing bulge luminosity. Hence, galaxies apparently become more efficient in producing radio emission relative to $H\alpha$ in bigger bulges. This also holds

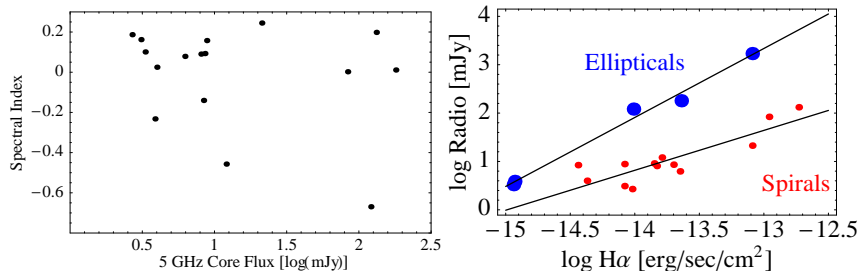


Figure 12: Left: Spectral indices of LLAGN in our two samples with $S_{15\text{GHz}} > 3$ mJy between 5 GHz (VLBI) and 15 GHz (VLA) as a function of radio core flux at 5 GHz. Right: $S_{15\text{GHz}}$ plotted versus narrow H α flux for the same sample; ellipticals and spirals are distinguished by big and small dots respectively.

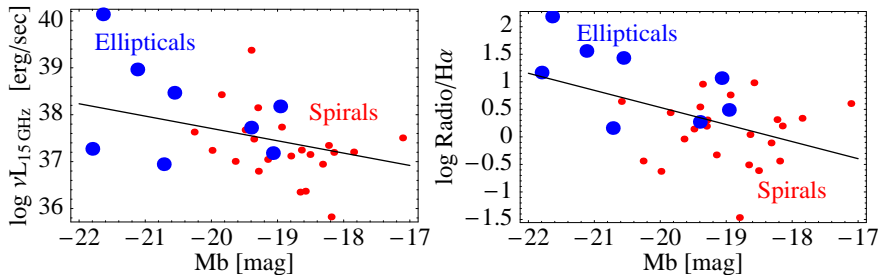


Figure 13: Left: Radio luminosity (νL_{ν}) at 15 GHz of LLAGN in our sample with $S_{15\text{GHz}} > 1.5$ mJy as a function of blue bulge magnitude. Right: Ratio between 15 GHz radio core and narrow H α flux as a function of blue bulge magnitude in the same sample. Ellipticals and spirals are distinguished by big and small dots respectively.

if we look at the entire VLA detected sample (Fig. 13). Whether this is due to increasing obscuration, effects intrinsic to the AGN, or a selection effect is unclear. In any case, we may be comparing pumpkins with apples. Since ellipticals and spirals in our sample are nicely separated between the top and bottom end of the bulge luminosity distribution, an apparent dichotomy in Fig. 12 is a natural consequence of this trend.

If the bulge luminosity is proportional to the central black hole mass (Kormendy & Richstone 1995; Ferrarese & Merritt 2000; Gebhardt et al. 2000), the ellipticals in our sample are more likely to have larger black hole masses. This means they have a larger ‘headroom’ with respect to their Eddington limit and are more likely to have larger accretion rates. Moreover, if an accretion disk becomes radiatively less efficient the further away it is from the Eddington limit, we could reproduce the scaling of the Radio/H α -ratio. Another explanation for the latter could be that the larger bulges of these ellipticals contain more obscuring material towards our line of sight and hence optical emission is more strongly suppressed.

To summarize: we find that at least 40% of optically selected LLAGN with Seyfert and LINER spectra have compact radio cores. VLBI observations

show that these cores are similar to radio jets in more luminous AGN with high brightness temperatures, jet-like structures, and flat radio spectra. The radio emission seems to be related to the luminosity of the emission-line gas and hence both are probably powered by genuine AGN operating at low powers. We found no evidence for high frequency components with highly inverted spectra as predicted in ADAF models. Hence, for these models one should probably not include radio fluxes in broad-band spectral fits.

We also find only a weak correlation between radio and bulge luminosity, which could imply a scaling of radio emission with black hole masses. Such an effect was claimed earlier and interpreted within the ADAF models as a possibility to measure black hole masses with the radio data (Franceschini, Vercellone, & Fabian 1998). However, this result was based on a much smaller, ill-selected sample and gave a much steeper dependence which we cannot confirm. As we have seen here, the radio- $H\alpha$ correlation is a much stronger effect. If the $H\alpha$ is a tracer of the accretion disk luminosity, this most likely means that the radio power is much more dependent on the accretion rate than on the black hole mass. One will therefore have to continue to measure black hole masses in the traditional way, mainly through spectroscopy.

5 Summary

Radio jets are the “smoking guns” of active galactic nuclei (AGN). They are also the site of many high-energy processes, including X-ray and γ -ray emission as well as high-energy particle acceleration. Early on it was the radio emission from these jets which drew people’s attention to quasars and led to their discovery. Today we know that radio jets are relativistic, magnetized plasma flows ejected at velocities close to the speed of light most likely from the immediate vicinity of black holes. At the smallest scales, the radio emission from these jets appears as very compact radio cores with a flat and variable radio spectrum. With Very Long Baseline Interferometry this emission can often be resolved into a core-jet structure sometimes showing apparent superluminal motion caused by the relativistic ejection velocity.

However, similar radio cores have also been found in quite a number of other sources, including the center of the Milky Way (Sgr A*), X-ray binaries (stellar mass black holes and neutron stars; see also Markoff, Falcke, & Fender 2000; Fender & Hendry 2000), and some nearby galaxies. Despite being interesting in their own right, none of these sources can compare in their power output and violence with quasars. On the other hand it is thought that in all these cases black holes (and in a few cases also neutron stars) are involved as well, possibly accreting at much lower levels – in absolute terms – than quasars.

Here we have discussed how these low-luminosity radio cores are related to their much more powerful siblings in quasars, radio galaxies, and Blazars. It is suggested that all radio cores can be described in a very similar fashion as jets coupled to an accretion disk (standard- α or ADAF), with jet and disk

being symbiotic features in an accretion scenario of black holes. At some level every black hole will accrete material but only a minority of sources reach the enormous power levels of quasars. The “silent majority” of black holes therefore operates at much lower levels producing much fainter radio cores.

Based on this idea of a “jet-disk symbiosis” a general emission model for radio cores can be derived which describes the radio emission of a collimated relativistic plasma flow after leaving its collimation region – the nozzle. This part of the jet is most likely dominated entirely by free expansion and is relatively independent of environmental influences. This leads to a relatively homogeneous appearance of compact radio cores in different sources with the jet power or the accretion rate being the main parameter. Such a model can explain sizes, fluxes, and spectra of many radio cores in weakly active black holes, such as Sgr A* in the Galactic Center or other Low-Luminosity AGN.

To conclude, one can say that the production of a relativistic jets seems to be an inevitable consequence of accreting black holes and is possible even at very low accretion rates. Therefore, compact radio cores are an ideal tracer of black holes in the near and distant universe. With the increasingly higher resolution and sensitivity of radio interferometers, they allow an intimate look at how black holes work at various scales and in different contexts.

Danksagungen

Ich möchte mich ganz herzlich bei dem Vorstand der Astronomischen Gesellschaft, insbesondere bei dem Vorsitzenden Herrn Prof. Sedlmayr, für die Verleihung des Ludwig-Biermann-Preises und die Einladung nach Bremen bedanken. Ebenso möchte ich an dieser Stelle den Herren Dr. Anton Zensus und Prof. Dr. Peter L. Biermann für ihre Unterstützung und Förderung in den letzten Jahren danken.

Herzlich danke ich auch meinen Kollegen, die zu den hier vorgestellten Arbeiten wesentlich beigetragen haben: Dr. Geoffrey Bower, Dr. Sera Markoff, Dr. Eric Agol, Prof. Fulvio Melia, Dr. Neil Nagar und Prof. Andrew Wilson. Diese Arbeit ist eine stark verkürzte und überarbeitete Fassung meiner gleichnamigen Habilitationsschrift. Dort ist auch eine umfassende Liste zugrundeliegender Originalarbeiten (soweit erschienen) sowie eine deutschsprachige Zusammenfassung zu finden.

REFERENCES

- Aitken, D. K., Greaves, J., Chrysostomou, A., Jenness, T., Holland, W., Hough, J. H., Pierce-Price, D., & Richer, J. 2000, *ApJ*, 534, L173
- Alonso-Herrero, A., Rieke, M. J., Rieke, G. H., & Shields, J. C. 2000, *ApJ*, 530, 688

- Backer, D. C., & Sramek, R. A. 1999, *ApJ*, 524, 805
- Backer, D. C., Zensus, J. A., Kellermann, K. I., Reid, M., Moran, J. M., & Lo, K. Y. 1993, *Science*, 262, 1414
- Baganoff, F., Bautz, M., Brandt, N., Cui, W., Doty, J., Feigelson, E., Garmire, G., Maeda, Y., Morris, M., Pravdo, S., Ricker, G., & Townsley, L. 2001, *ApJ*, submitted
- Balick, B., & Brown, R. L. 1974, *ApJ*, 194, 265
- Bardeen, J. M. 1973, in *Black Holes*, ed. C. DeWitt & B. S. DeWitt (New York: Gordon & Breach), 215
- Barth, A. J., Ho, L. C., Filippenko, A. V., & Sargent, W. L. W. 1998, *ApJ*, 496, 133
- Beckert, T., & Duschl, W. J. 1997, *A&A*, 328, 95
- Bietenholz, M. F., et al. 1996, *ApJ*, 457, 604
- Blandford, R. D., & Königl, A. 1979, *ApJ*, 232, 34
- Boroson, T. A., & Green, R. F. 1992, *ApJS*, 80, 109
- Bower, G. C., & Backer, D. C. 1998, *ApJ*, 496, L97
- Bower, G. C., Backer, D. C., Zhao, J. H., Goss, M., & Falcke, H. 1999a, *ApJ*, 521, 582
- Bower, G. C., Falcke, H., & Backer, D. C. 1999, *ApJ*, 523, L29
- Bower, G. C., Wright, M. C. H., Backer, D. C., & Falcke, H. 1999b, *ApJ*, 527, 851
- Bridle, A. H., Hough, D. H., Lonsdale, C. J., Burns, J. O., & Laing, R. A. 1994, *AJ*, 108, 766
- Bridle, A. H., & Perley, R. A. 1984, *ARA&A*, 22, 319
- Brunthaler, A., Falcke, H., Bower, G. C., Aller, M. F., Aller, H. D., Teräsranta, H., Lobanov, A. P., Krichbaum, T. P., & Patnaik, A. R. 2000, *A&A*, 357, L45
- Chevalier, R. A. 1992, *ApJ*, 397, L39
- Coker, R., Melia, F., & Falcke, H. 1999, *ApJ*, 523, 642
- Coker, R. F., & Melia, F. 1997, *ApJ*, 488, L149
- Cotton, W. D., Wittels, J. J., Shapiro, I. I., Marcaide, J., Owen, F. N., Spangler, S. R., Rius, A., Angulo, C., Clark, T. A., & Knight, C. A. 1980, *ApJ*, 238, L123

- Cunningham, C. T. 1975, *ApJ*, 202, 788
- Davies, R. D., Walsh, D., & Booth, R. S. 1976, *MNRAS*, 177, 319
- Doeleman, S., Rogers, A. E. E., Backer, D. C., Wright, M., & Bower, G. C. 1999, in *ASP Conf. Ser. 186: The Central Parsecs of the Galaxy*, ed. H. Falcke, A. Cotera, W. Duschl, F. Melia, & M. J. Rieke (San Francisco: Astronomical Society of the Pacific), 98
- Doeleman, S. S., Shen, Z., Rogers, A. E. E., Bower, G. C., Wright, M. C. H., Zhao, J. H., Backer, D. C., Crowley, J. W., Freund, R. W., Ho, P. T. P., Lo, K. Y., & Woody, D. P. 2001, *AJ*, 121, 2610
- Donea, A. C., & Biermann, P. L. 1996, *A&A*, 316, 43
- Duschl, W. J., & Lesch, H. 1994, *A&A*, 286, 431
- Eckart, A., & Genzel, R. 1996, *Nature*, 383, 415
- Eckart, A., & Genzel, R. 1997, *MNRAS*, 284, 576
- Eckart, A., Genzel, R., Hofmann, R., Sams, B. J., & Tacconi-Garman, L. E. 1993, *ApJ*, 407, L77
- Faber, S. M., Tremaine, S., Ajhar, E. A., Byun, Y. I., Dressler, A., Gebhardt, K., Grillmair, C., Kormendy, J., Lauer, T. R., & Richstone, D. 1997, *AJ*, 114, 1771
- Falcke, H. 1996, in *IAU Symp. 169: Unsolved Problems of the Milky Way*, ed. L. Blitz & P. Teuben, Vol. 169 (Dordrecht: Kluwer), 169
- Falcke, H., & Biermann, P. L. 1995, *A&A*, 293, 665
- Falcke, H., & Biermann, P. L. 1996, *A&A*, 308, 321
- Falcke, H., & Biermann, P. L. 1999, *A&A*, 342, 49
- Falcke, H., Gopal-Krishna, & Biermann, P. L. 1995, *A&A*, 298, 395
- Falcke, H., Goss, W. M., Matsuo, H., Teuben, P., Zhao, J. H., & Zylka, R. 1998, *ApJ*, 499, 731
- Falcke, H., & Heinrich, O. M. 1994, *A&A*, 292, 430
- Falcke, H., Malkan, M. A., & Biermann, P. L. 1995, *A&A*, 298, 375
- Falcke, H., Mannheim, K., & Biermann, P. L. 1993, *A&A*, 278, L1
- Falcke, H., & Markoff, S. 2000, *A&A*, 362, 113
- Falcke, H., & Melia, F. 1997, *ApJ*, 479, 740

- Falcke, H., Melia, F., & Agol, E. 2000a, in *Cosmic Explosions*, 10th Astrophysics Conference, College Park, Maryland, AIP Conf. Ser., Vol. 522, ed. S. Holt & W. Zhang (Melville, New York: AIP), 317
- Falcke, H., Melia, F., & Agol, E. 2000b, *ApJ*, 528, L13
- Falcke, H., Nagar, N. M., Wilson, A. S., & Ulvestad, J. S. 2000, *ApJ*, 542, 197
- Falcke, H., Sherwood, W., & Patnaik, A. R. 1996, *ApJ*, 471, 106
- Fender, R. P., & Hendry, M. A. 2000, *MNRAS*, 317, 1
- Ferrarese, L., & Merritt, D. 2000, *ApJ*, 539, L9
- Filippenko, A. V., & Terlevich, R. 1992, *ApJ*, 397, L79
- Franceschini, A., Vercellone, S., & Fabian, A. C. 1998, *MNRAS*, 297, 817
- Gallimore, J. F., Baum, S. A., & O’Dea, C. P. 1997, *Nature*, 388, 852
- Gebhardt, K., et al. 2000, *ApJ*, 539, L13
- Ghez, A. M., Klein, B. L., Morris, M., & Becklin, E. E. 1998, *ApJ*, 509, 678
- Ghez, A. M., Morris, M., Becklin, E. E., Tanner, A., & Kremenek, T. 2000, *Nature*, 407, 349
- Gwinn, C. R., Danen, R. M., Tran, T. K., Middleditch, J., & Ozernoy, L. M. 1991, *ApJ*, 381, L43
- Haller, J. W., Rieke, M. J., Rieke, G. H., Tamblyn, P., Close, L., & Melia, F. 1996, *ApJ*, 456, 194
- Hazard, C., Mackey, M. B., & Shimmins, A. J. 1963, *Nature*, 197, 1037
- Heckman, T. M. 1980, *A&A*, 87, 152
- Heckman, T. M., van Breugel, W., Miley, G. K., & Butcher, H. R. 1983, *AJ*, 88, 1077
- Ho, L. C. 1999, *ApJ*, 516, 672
- Ho, L. C., Filippenko, A. V., & Sargent, W. L. 1995, *ApJS*, 98, 477
- Ho, L. C., Filippenko, A. V., & Sargent, W. L. W. 1997, *ApJS*, 112, 315
- Jaroszynski, M., & Kurpiewski, A. 1997, *A&A*, 326, 419
- Kellermann, K. I., Sramek, R., Schmidt, M., Shaffer, D. B., & Green, R. 1989, *AJ*, 98, 1195
- Klein, U., Mack, K. H., Strom, R., Wielebinski, R., & Achatz, U. 1994, *A&A*, 283, 729

- Köhler, T., Groote, D., Reimers, D., & Wisotzki, L. 1997, *A&A*, 325, 502
- Kormendy, J., & Richstone, D. 1995, *ARA&A*, 33, 581
- Krichbaum, T. P., Graham, D. A., Witzel, A., Greve, A., Wink, J. E., Grewing, M., Colomer, F., de Vicente, P., Gomez-Gonzalez, J., Baudry, A., & Zensus, J. A. 1998, *A&A*, 335, L106
- Krichbaum, T. P., et al. 1993, *A&A*, 274, L37
- Lo, K. Y., Shen, Z. Q., Zhao, J. H., & Ho, P. T. P. 1998, *ApJ*, 508, L61
- Lüst, R. 1952, *Zeitschrift f. Naturf.*, 7a, 87
- Lynden-Bell, D., & Pringle, J. E. 1974, *MNRAS*, 168, 603
- Lynden-Bell, D., & Rees, M. J. 1971, *MNRAS*, 152, 461
- Magorrian, J., Tremaine, S., Richstone, D., Bender, R., Bower, G., Dressler, A., Faber, S. M., Gebhardt, K., Green, R., Grillmair, C., Kormendy, J., & Lauer, T. 1998, *AJ*, 115, 2285
- Mahadevan, R. 1998, *Nature*, 394, 651
- Maoz, D., Filippenko, A. V., Ho, L. C., Macchetto, F. D., Rix, H. W., & Schneider, D. P. 1996, *ApJS*, 107, 215
- Markoff, S., Falcke, H., & Fender, R. 2000, preprint, astro
- Marti, J. M. A., Mueller, E., Font, J. A., Ibanez, J. M. A., & Marquina, A. 1997, *ApJ*, 479, 151
- Mastichiadis, A., & Ozernoy, L. M. 1992, in *American Astronomical Society Meeting*, Vol. 181, 10904
- Melia, F. 1992, *ApJ*, 387, L25
- Melia, F. 1994, *ApJ*, 426, 577
- Melia, F., & Falcke, H. 2001, *ARA&A*, 39, submitted
- Melia, F., Jokiipii, J. R., & Narayanan, A. 1992, *ApJ*, 395, L87
- Menten, K. M., Reid, M. J., Eckart, A., & Genzel, R. 1997, *ApJ*, 475, L111
- Mezger, P. G., Duschl, W. J., & Zylka, R. 1996, *A&A Rev.*, 7, 289
- Miller, P., Rawlings, S., & Saunders, R. 1993, *MNRAS*, 263, 425
- Miyoshi, M., Moran, J., Herrnstein, J., Greenhill, L., Nakai, N., Diamond, P., & Inoue, M. 1995, *Nature*, 373, 127
- Morris, M., & Serabyn, E. 1996, *ARA&A*, 34, 645

- Nagar, N. M., Falcke, H., Wilson, A. S., & Ho, L. C. 2000, *ApJ*, 542, 186
- Narayan, R., Mahadevan, R., Grindlay, J. E., Popham, R. G., & Gammie, C. 1998, *ApJ*, 492, 554
- Narayan, R., & Yi, I. 1994, *ApJ*, 428, L13
- Narayan, R., & Yi, I. 1995a, *ApJ*, 444, 231
- Narayan, R., & Yi, I. 1995b, *ApJ*, 452, 710
- Narayan, R., Yi, I., & Mahadevan, R. 1995, *Nature*, 374, 623
- Narayan, R., Yi, I., & Mahadevan, R. 1996, *A&AS*, 120, C287
- Neugebauer, G., Green, R. F., Matthews, K., Schmidt, M., Soifer, B. T., & Bennett, J. 1987, *ApJS*, 63, 615
- O'Connell, R. W., & Dressel, L. L. 1978, *Nature*, 276, 374
- Ozernoy, L. 1992, in *Testing the AGN Paradigm*, AIP Conf. Proc. 254, ed. C. M. U. S. S. Holt, S. G. Neff (New York: AIP), 40
- Perez-Fournon, I., & Biermann, P. 1984, *A&A*, 130, L13
- Predehl, P., & Trümper, J. 1994, *A&A*, 290, L29
- Rawlings, S., & Saunders, R. 1991, *Nature*, 349, 138
- Rees, M. J. 1982, in *AIP Conf. Proc. 83: The Galactic Center*, ed. G. R. Riegler & R. D. Blandford (New York: American Institute of Physics), 166
- Rees, M. J. 1984, *ARA&A*, 22, 471
- Reid, M. J., Readhead, A. C. S., Vermeulen, R. C., & Treuhaft, R. N. 1999, *ApJ*, 524, 816
- Reuter, H. P., & Lesch, H. 1996, *A&A*, 310, L5
- Richstone, D., et al. 1998, *Nature*, 14
- Rogers, A. E. E., Doeleman, S., Wright, M. C. H., Bower, G. C., Backer, D. C., Padin, S., Philips, J. A., Emerson, D. T., Greenhill, L., Moran, J. M., & Kellermann, K. I. 1994, *ApJ*, 434, L59
- Ruffert, M., & Melia, F. 1994, *A&A*, 288, L29
- Schlickeiser, R., Campeanu, A., & Lerche, L. 1993, *A&A*, 276, 614
- Schmidt, M. 1963, *Nature*, 197, 1040
- Schmidt, M., & Green, R. F. 1983, *ApJ*, 269, 352

- Schneider, P. 1993, *A&A*, 278, 315
- Serabyn, E., Carlstrom, J., Lay, O., Lis, D. C., Hunter, T. R., & Lacy, J. H. 1997, *ApJ*, 490, L77
- Shakura, N. I., & Sunyaev, R. A. 1973, *A&A*, 24, 337
- Slee, O. B., Sadler, E. M., Reynolds, J. E., & Ekers, R. D. 1994, *MNRAS*, 269, 928
- Strittmatter, P. A., Hill, P., Pauliny-Toth, I. I. K., Steppe, H., & Witzel, A. 1980, *A&A*, 88, L12
- Subrahmanyan, R., & Saripalli, L. 1993, *MNRAS*, 260, 908
- Sun, W. H., & Malkan, M. A. 1989, *ApJ*, 346, 68
- Thorne, K. S. 1981, *MNRAS*, 194, 439
- Urry, C. M., & Padovani, P. 1995, *PASP*, 107, 803
- van Dyk, S. D., & Ho, L. C. 1998, in *IAU Symp. 184: The Central Regions of the Galaxy and Galaxies*, Vol. 184, 489
- van Langevelde, H. J., Frail, D. A., Cordes, J. M., & Diamond, P. J. 1992, *ApJ*, 396, 686
- Viergutz, S. U. 1993, *A&A*, 272, 355
- von Weizsäcker, C. F. 1948, *Zeitschrift f. Naturf.*, 3a, 524
- Wright, M. C. H., & Backer, D. C. 1993, *ApJ*, 417, 560
- Wrobel, J. M., & Heeschen, D. S. 1984, *ApJ*, 287, 41
- Yuan, F. 2000, *MNRAS*, 319, 1178
- Yusef-Zadeh, F., Cotton, W., Wardle, M., Melia, F., & Roberts, D. A. 1994, *ApJ*, 434, L63
- Yusef-Zadeh, F., & Morris, M. 1991, *ApJ*, 371, L59
- Zirbel, E. L., & Baum, S. A. 1995, *ApJ*, 448, 521
- Zylka, R., Mezger, P. G., & Lesch, H. 1992, *A&A*, 261, 119
- Zylka, R., Mezger, P. G., Ward-Thompson, D., Duschl, W. J., & Lesch, H. 1995, *A&A*, 297, 83